Computers and Chemical Engineering 115 (2018) 455–473

Contents lists available at ScienceDirect

Computers and Chemical Engineering

journal homepage: www.elsevier.com/locate/compchemeng

Security constrained unit commitment scheduling: A new MILP formulation for solving transmission constraints

Gonzalo E. Alvarez[a], Marian G. Marcovecchio[a,b], Pío A. Aguirre[a,b,*]

[a] INGAR/CONICET-UTN, Instituto de Desarrollo y Diseño, Santa Fe, Argentina
[b] UNL, Universidad Nacional del Litoral, Santa Fe, Argentina

ARTICLE INFO

Article history:
Received 19 December 2017
Revised 24 March 2018
Accepted 4 May 2018
Available online 12 May 2018

Keywords:
Transmission constraints
Mixed integer linear programming
Power system scheduling
Optimization

ABSTRACT

This paper presents a new Mixed Integer Linear Programming model (MILP) to account for the Security-Constrained Unit Commitment Problem (SCUC). Transmission Constraints are introduced through bus balances, line power bound flows, and bus voltage angle differences. Line status is also considered. Binary variables regarding line status (active or inactive) are introduced for this purpose.

These variables allow discrete decisions on the connectivity of buses, reducing the angle coupling between buses, with several advantages.

Three examples are solved. The results indicate that this method can obtain feasible solutions with CPU times of 2.5 s (for a 6-bus system) and 500 s (for the IEEE 118-bus system), and they reached cost savings up to 4.9% of the total generating cost for one day of programming horizon, in comparison with classical models.

Relations of the network are illustrated graphically, and an analysis of the results is presented through new evaluation indexes.

1. Introduction

Near 80% of the energy consumed in the world comes from the combustion produced by fossil fuels, including 31.4% from oil, 29.0% from coal, and 21.3% from natural gas (International Energy Agency, 2014). Countries economic growth depends, among other factors, on energy availability at low costs. The current way of producing energy is hard to sustain due to two main reasons. First, the environmental impacts (Saidi & Hammami, 2015). Second, the decrease of fossil fuel reserves (Shafiee & Topal, 2009): some of the new fossil fuel reserves are located in difficult to access areas; this means that fossil fuels will be available only after paying expensive extraction processes. The “renewable way” is in constant progress and depends on geographical factors. Improving energy efficiency of electric power systems is a global issue, independent of geographical factors.

A growing interest in the optimal design and operation of complex generation, transmission and distribution systems is the subject of this work. The problem of operation involves several subproblems, being scheduling of generating units one of the most recognized due to the economic and environmental advantages that can be derived from optimization. Scheduling of generating units to meet a forecast demand in an efficient manner, is known as Unit Commitment (UC) problem (Lowery, 1966).

The objective of the UC problem is to minimize the operating costs by an optimal schedule of power generators along a predefined time horizon. Time horizons range from 24 h to one week. Different constraints are considered according to the set of units involved (Oonsivilai, Marungsri, Barsoum, Uatrongjit, & Vasant, 2008; Wright, 2013): spinning reserve, lower and upper bounds on power, minimum up/down time and ramp limits.

Many approaches have been developed by different authors to solve this problem. Most methods for solving UC problem can be grouped into two broad categories: deterministic techniques and heuristic techniques. Deterministic methods include Priority List, Dynamic Programming, Integer and Linear Programming, Branch and Bound, Lagrangian Relaxation, and others. While heuristic methods include Tabu Search, Simulated Annealing, Expert Systems, Fuzzy Systems, Artificial Neural Networks, Genetic Algorithms, Evolutionary Programming, Ant Colony Search Algorithm, Hybrid Models, and others (Padhy, 2004).

Mathematical programming is a widely used approach in decision-making processes. Within the scope of Mathematical Programming, Mixed Integer Linear Programming (MILP) is experiencing a rapid grow in solving technical processes due to the advantages of linear models (Vielma, 2015).

* Corresponding author at: INGAR/CONICET-UTN, Avellaneda 3657, S3002GJC Santa Fe, República Argentina.
E-mail address: paguir@santafe-conicet.gov.ar (P.A. Aguirre).

https://doi.org/10.1016/j.compchemeng.2018.05.001
0098-1354/

Nomenclature

Indexes

i	unit index
t	time period index
l	transmission line index
bu	bus index
c	load index
bu_i	power input bus index
bu_o	power output bus index

Constants

a_i, b_i,c_i,	coefficients of fuel cost function for unit i *($/MWh^2), ($/MWh),($)*
I	total number of units
T	total number of periods
R_t	spinning reserve required for time period t *(MW)*
p_i^{LO}	lower limit of power generation of unit i *(MW)*
p_i^{UP}	upper limit of power generation of unit i *(MW)*
T_i^{ini}	initial status of unit i *(h)*
TD_i	minimum OFF time of unit i *(h)*
TU_i	minimum ON time of unit i (h)
DR_i	ramp-down rate limit of unit i *(MW/h)*
UR_i	ramp-up rate limit of unit i *(MW/h)*
SD_i	maximum shutdown rate of unit i *(MW)*
SU_i	maximum startup rate of unit i *(MW)*
Hsc_i	hot start costs of unit i *($)*
Csc_i	cold starts costs of unit i *(h)*
TD_i^{cold}	cold start hours of unit i *(h)*
DC_i	shut down costs for unit i *($)*
$bkt_{c,\ bu,\ t}$	load requirement at load c, bus bu, and time t *(MW)*
x_l	reactance of line l (p.u.)
r_l	resistance of line l (p.u.)
$\overline{F_l}$	real power flow limit on transmission line l (MW)
L	total number of transmission lines
BU	total number of Buses
C	total number of Loads
$g_{bu_i bu_o}$	susceptance of transmission line connecting the bus bu_i with the bus bu_o *(p.u.)*
$b_{bu_i bu_o}$	conductance of transmission line connecting the bus bu_i with the bus bu_o (p.u.)
$\Gamma_{l,\ i}$, $\Gamma_{l,\ c}$	matrixes relating to the power flows on transmission line l with the generator output i or load c
$t.a._i$	active time. Hour that the unit i is generating power (h)

Variables

$u_{i,\ t}$	binary variable: 1 if unit i is on, 0 if unit i is off, at time t
$p_{i,\ t}$	power output of unit i at time period t (MW)
$cu_{i,\ t}$	startup cost of unit i at time period t *($)*
$cd_{i,\ t}$	shut down cost of unit i at time period t *($)*
$p\_l_{l,bu_i,bu_o,t}$	real power flow of line l (MW)
$q\_l_{l,bu_i,bu_o,t}$	reactive power flow of line l, input bus bui and output bus buo, and time t (MVAR)
V_{bu}	voltage in bus bu (MV)
θ_{bu}	voltage angle in bus bu (rad)
$\theta_{bu_i bu_o}$	difference of bus voltage angles between connected buses (rad)
$y_{l,\ t}$	binary variable: Status of line l and time t

Transmission constraints are important in the formulation of UC problem, because they ensure that centers of consumption are properly supplied by the power plants. Solutions of classical Unit Commitment Problem could lead to forbidden operating regions of the system (Guan, Zhai, & Papalexopoulos, 2003; Kazarlis, Bakirtzis, & Petridis, 1996; Ostrowski, Anjos, & Vannelli, 2012; Quan, Srinivasan, Khambadkone, & Khosravi, 2015; Zhai, Guan, & Yang, 2009). When the works do not consider transmission constraints into the model, that could lead to several problems such as line overloads, or even that the systems are unable to transmit the programmed generation. When transmission constraints are considered and added to the UC problem, it is known as Security-Constrained Unit Commitment Problem (SCUC). This approach provides an efficient and workable schedule which is more appropriated for a real electric system.

Plenty of methods have been proposed to solve transmission constraints in Security-Constrained Unit Commitment Problems (Abdul-Rahman, Shahidehpour, Aganacic, & Mokhtari, 1996; Castillo, Conejo, Pedregal, Garcia, & Alguacil, 2002; Fu, Shahidehpour, & Li, 2005; Guan *et al.*, 2005; Reza Norouzi, Ahmadi, Esmaeel Nezhad, & Ghaedi, 2014; Senthil Kumar & Mohan, 2010; Tseng et al., 1999; Wang, Shahidehpour, Li, & Member, 2009; Yamin, 2004; Zhao, Luh, Yan, Stern, & Chang, 2008), and have been applied to complex systems (Guy, 1971; Ruzic & Rajakovic, 1991). In 1995, Shaw introduced a method which solve transmission constraints trough Lagrangian relaxation (Shaw, 1995). The Direct Method was presented and lower-cost solutions were obtained compared with so-called Indirect Methods.

In the literature two models are mainly adopted to represent transmission limits: AC power flow and DC power flow.

The AC power flow model is characterized by the high accuracy and detailed level of results, however obtaining an optimal solution using this model could be time consuming, especially in real large-scale power systems.

In real power markets analysis, the requirement of calculation speed is of most concern, comparing with the requirement of calculation precision (Zhu, 2009). DC power flow model (Tseng, Guan, & Svoboda, 1998) is an approximation of AC power flow and its main advantage is the reduction of computational requirements due to the use of linear equations, with an acceptable level of accuracy (Overbye, Cheng, & Sun, 2004; Stott, Jardim, & Alsac, 2009).

This paper presents a new approach for modeling the SCUC problem, based on the UC formulation developed in (Marcovecchio, Novais, & Grossmann, 2014), with the aim to solve the model though deterministic optimization. Transmission constraints presented in this paper are based on DC model. The goal of this work is the implementation of binary variables for line status to model transmission constraints, discriminating between active and inactive lines. In this approach, the differences of the voltage angle between buses depend on the power flow circulation through lines that connect these buses. By implementing this model, it is possible to represent more solutions compared to classical models. Then, lower operating costs could be reached. In fact, variables of bus voltage angles can take wider ranges of values due to the implementation of the proposed binary variables. Implementing the proposed model, SCUC problems can be solved in efficient computational times without implementing loops matrixes as is done in other formulations (Stagg & El-Abiad, 1968; Yan & Sekar, 2005).

Works like Fu et al. (2005) and Wang et al. (2009), include transmission constraints using AC power flow model, but this model does not decouple buses when there not power flow in the associated transmission lines. On the other hand, Reza Norouzi et al. (2014); Senthil Kumar and Mohan (2010); Yamin (2004) and Zhao et al. (2008) implement the DC power flow model, but the model does not distinguish between active or inactive lines. Other works like Abdul-Rahman et al. (1996), Guan, Guo, and Zhai (2005) and Tseng et al. (1999) do not consider the voltage bus angle constraints at all.

With the aim of illustrating the effectiveness of the proposed modeling, three systems are tested: a 6-bus system, a 31-bus system, and the IEEE 118–bus system. First, each UC problem is studied using CPLEX and Gurobi which are the most commonly used solvers. Then SCUC problems are tested modeling transmission constraints without the proposed binary variables, as in the classical model formulation. In third place, the three systems are studied, including the proposed binary variables for modeling transmission constraints and results are compared to previous cases. Comparisons between solvers are presented.

Another contribution of this paper is the implementation of graphs to illustrate the obtained results. Graphs illustrate the status of lines and buses, according to their relative contribution to the network. The proposed approach shows not only how to operate the system in a more efficient way, but also indicates where to emphasize maintenance and investments for renovation and expansion of networks for the companies responsible of the system operations.

The rest of this paper is organized as follows. The basic UC problem is mathematically formulated in Section II. The new approach for solving transmission constraints is introduced in Section III. Numerical examples are shown in Section IV for illustrating the performance of the proposed model. Analyses of the results obtained are presented in Section V. Finally, Section VI draws the conclusion of this work.

2. UC problem formulation

The Unit Commitment problem (UC) consists in determining the most economical scheduling of generating units with the aim of meeting a forecast demand. The UC problem is formulated as a mathematical programming model, whose objective function to be minimized is the power system operating cost. It includes the cost of the fuel consumed which is estimated by a quadratic function, together with fixed startup ($cu_{i,\,t}$) and shutdown costs ($cd_{i,\,t}$) of each unit over the time programming horizon (1). (Carrión & Arroyo, 2006; Marcovecchio et al., 2014). $u_{i,\,t}$ is a binary variable which indicate the ON/OFF status of the unit i.

The electric system is composed by I thermal units; and a_i, b_i, c_i are the coefficients for computing the fuel consumption cost when units are generating power ($p_{i,\,t} > 0$). There are C power loads that represent the demand, L transmission lines, and BU buses where the generators, loads, or lines are located. The programming horizon includes T hours.

Moreover, i is the set for generating units, c is the set for power loads, l is the set for transmission lines, bu is the set for busses, and t is the set for time periods.

$$\min C = \sum_{i=1}^{I}\sum_{t=1}^{T}\left[\left(a_i u_{i,t} + b_i p_{i,t} + c_i {p_{i,t}}^2\right) + cu_{i,t} + cd_{i,t}\right] \quad (1)$$

Where $p_{i,\,t}$ is the power generated by unit i during the time period t, and $u_{i,\,t}$ is a binary variable which indicates the ON/OFF status of unit i at each time period.

With the aim of obtaining a MILP formulation, the quadratic terms of the objective function (1) will be linearly underestimated. Eqs. (2)–(20) are the constraints to be satisfied.

The forecast demand of power to be met:

$$\sum_{c=1}^{C}\sum_{bu=1}^{BU} bkt_{c,bu,t} \le \sum_{i=1}^{I} p_{i,t}, \;\; t = 1, \;\ldots, T \quad (2)$$

Spinning reserve (R_t) is the on-line generation capacity that is unloaded, but available by increasing the power output of units that are already connected to the power system. It can respond quickly to compensate outages.

$$\sum_{c=1}^{C}\sum_{bu=1}^{BU} bkt_{c,bu,t} + R_t \le \sum_{i=1}^{I} p_i^{UP} u_{i,t}, \quad t = 1, \;\ldots, T \quad (3)$$

Each unit has a minimum and maximum limit of real power generation:

$$u_{i,t}\; p_i^{LO} \le p_{i,t} \le u_{i,t}\; p_i^{UP}, \;\; t = 1, \quad \ldots, T; i = 1, \ldots, I \quad (4)$$

The initial status (T_i^{ini}) indicates the number of hours that each unit has been online/offline before the beginning of the programming horizon. And, the minimum UP/DOWN time is the number of hours that each unit must remain in ON/OFF status, once it is turned ON/OFF.

Thus, initial status and minimum UP/DOWN times (TU_i/TD_i) determinate the ON/OFF status of each unit at its earliest operating periods.

$$u_{i,t} = 0 \;\forall i : T_i^{ini} < 0; \;\; t = 1, \ldots.. \left(TD_i + T^{ini}\right) \quad (5)$$

$$u_{i,t} = 1 \;\forall i : T_i^{ini} > 0; \;\; t = 1, \ldots.. \left(TU_i - T^{ini}\right) \quad (6)$$

If $T_i^{ini} > 0$, it indicates the amount of hours that unit i was online before the first hour of the programing horizon. Similarly, if $T_i^{ini} < 0$, it indicates the number of hours that unit i was offline.

The number of hours that unit i must remain online/offline after it was turned ON/OFF is imposed by Eqs. (7)–(10):

$$u_{i,t} - u_{i,t-1} \le u_{i,t+j}, \quad i = 1, \ldots\ldots I; \; t = 2, \ldots\ldots T; \; j = 1, \ldots\ldots (TU_i - 1) \quad (7)$$

$$u_{i,1} \le u_{i,1+j}, \;\; \forall i : T_i^{ini} < 0; \;\; j = 1, \ldots.. \;(TU_i - 1) \quad (8)$$

$$u_{i,t+j} \le u_{i,t} - u_{i,t-1} + 1 \quad i = 1, \;\ldots\ldots I, \; t = 2, \;\ldots\ldots T; \, j = 1, \;\ldots\ldots (TD_i - 1) \quad (9)$$

$$u_{i,1+j} \le u_{i,1}, \qquad \forall i \;: T_i^{ini} > 0; \;\; j = 1, \;\ldots\ldots (TD_i - 1) \quad (10)$$

Ramp rate limits avoid possible unit damages due to an excessive increase or decrease in the power output. UR_i is a constant for the ramp ascending limit and DR_i is the ramp descending limit for the unit i. SU_i/SD_i are the maximum start-up/shut down rates.

$$p_{i,t-1} - DR_i u_{i,t} - SD_i(1 - u_{i,t}) \le p_{i,t}, \;\; i = 1, \ldots\ldots I; \;\; t = 2, \;\ldots\ldots T \quad (11)$$

$$p_{i,t} \le p_{i,t-1} + UR_i u_{i,t-1} - SU_i(1 - u_{i,t-1}), \;\; i = 1, \ldots\ldots I; t = 2, \;\ldots, T \quad (12)$$

The value of the variable *star up cost* depends of several technical characteristics of the generator. One of these characteristics is the amount of hours that the unit has been in OFF status before it turns ON (DOWN time) Naidoo, 2007). If the DOWN time $\le (TD_i + T_i^{cold})$, then the start-up cost is computed as the *hot start cost: Hsc_i*. If not, then it is computed as the *cold start cost: Csc_i*. Eqs. (13)–((17) define this cost function. T_i^{cold} is a constant that added to TD_i, is the number of down time hours limiting between *hot start cost* and *cold start cost.* The value of Csc_i is higher than the value of Hsc_i, because as time passes, the temperature of unit is lower and more fuel is required for starting it up.

The *hot start cost* is modeled by the following constraints:

$$(u_{i,t} - \; u_{i,t-1})\; Hsc_i \;\; \le cu_{i,t}, \;\; i = 1, \;\ldots, I; \;\; t = 2, \;\ldots, T \quad (13)$$

$$u_{i,1} Hsc_i \;\; \le cu_{i,t}, \;\; \forall i : T_i^{ini} < 0 \quad (14)$$

Similarly, the *cold start cost* is modeled mathematically by Eqs. (15) and (16) as follows:

$$\left(u_{i,t} - \sum_{j<TD_i+T_i^{cold}+1} u_{i,t-j}\right) Csc_i \le cu_{i,t}$$
$$i = 1, \ldots\ldots I;\ TD_i + T_i^{cold} < t \le T \quad (15)$$

$$\left(u_{i,t} - \sum_{j<t} u_{i,t-j}\right) Csc_i \le cu_{i,t},$$
$$\forall i\ : T_i^{ini} < 0;\ (TD_i + T_i^{cold} + 1) < t \le \left(TD_i + T_i^{cold}\right) \quad (16)$$

If unit i is not turned on at the time period t, Eq. (17) ensures that the value of start-up cost is equal to zero.

$$0 \le cu_{i,t},\ i = 1, \ldots, I;\ t = 1, \ldots, T \quad (17)$$

Occasionally, a shut-down cost must be imposed. This is modeled by Eqs. (18) and (19). $cd_{i,\,t}$ is the shut-down cost variable.

$$(u_{i,t-1} - u_{i,t})DC_i \le cd_{i,t},\ i = 1, \ldots, I;\ t = 2, \ldots, T \quad (18)$$

$$(1 - u_{i,1})DC_i \le cd_{i,t},\ \forall i : T_i^{ini} > 0; \quad (19)$$

In a similar way, Eq. (20) together with the optimization process, prevent the shutdown cost from taking negative values.

$$0 \le cd_{i,t}\ i = 1, \ldots\ldots I;\ t = 1, \ldots\ldots T \quad (20)$$

Eqs. (1)–(20) model the Unit Commitment Problem, when the transmission constraints are not considered. These constraints are discussed in the following section.

3. SCUC problem formulation

3.1. Formulation of transmission constraints using classic power flow models: AC and DC

By the inclusion of transmission constraints, models may incur in significant computational complexities due to variables representing power flows through the lines are annexed. When transmission constraints are included, the UC problem is known as Security-Constrained Unit Commitment Problem (SCUC). These constraints model the power flow of transmission network, in order to ensure the capacities of the lines are not exceeded. In (Shaw, 1995) the author introduced the following constraint to address transmission constraints:

$$-\overline{F_l} \le p_{ll,t} = \sum_{i=1}^{I} \Gamma_{l,i} p_{i,t} - \sum_{c=1}^{C} \sum_{bu=1}^{BU} \Gamma_{l,c} bkt_{c,bu,t} \le \overline{F_l},\ t = 1, \ldots, T \quad (21)$$

where $\Gamma_{l,\,i}$ and $\Gamma_{l,\,c}$ are the matrixes relating to the power flows on transmission line l with the generator output or load.

The AC power flow model is detailed in (Bai, Zhong, Xia, Kang, & Xie, 2015) and is briefly described in this section. Eq. (22) models the real power flow sent from bus bu_i to bus bu_o, and Eq. (23) represents the reactive power flow circulating from bus bu_i to bus bu_o.

$$p\_l_{bu_i-bu_o,t} = V_{bu_i} \sum_{bu_o=1}^{BU} V_{bu_o}\left(g_{bu_i,bu_o} Cos\theta_{bu_i-bu_o,t} + b_{bu_i,bu_o} Sin\theta_{bu_i-bu_o,t}\right)$$
$$bu_i = 1, \ldots, BU;\ bu_o = 1, \ldots, BU;\ t = 1, \ldots, T \quad (22)$$

$$q\_l_{bu_i-bu_o,t} = V_{bu_i} \sum_{bu_o=1}^{BU} V_{bu_o}\left(g_{bu_i,bu_o} Sin\theta_{bu_i-bu_o,t} - b_{bu_i,bu_o} Cos\theta_{bu_i-bu_o,t}\right)$$
$$bu_i = 1, \ldots, BU;\ bu_o = 1, \ldots, BU;\ t = 1, \ldots, T \quad (23)$$

A power system with BU buses results in an AC power flow model with 2*BU non-linear equations and 8*BU continuous variables. As a consequence, the major difficulty of the AC power flow model is the computational effort required for its resolution. Therefore, a simplified lineal model based on the AC power flow one has been developed for Unit Commitment problem: DC power flow model. The DC power flow model described in this section is based on (Alvarez, Marcovecchio, & Aguirre, 2016; Van Den Bergh, Delarue, & D'haeseleer, 2014; Zhu, 2009). This model only considers active power flows and supposes transmission losses as negligible.

The DC power flow model is based on the following three assumptions:

1 Voltage angle differences $\theta_{bu_i-bu_o}$ between neighboring buses are small enough, such that the sine and cosine terms in the AC power flow model can be approximated linearly as follows:

$$Sin\ \theta_{bu_i-bu_o} \cong \theta_{bu_i-bu_o} \quad (24)$$

$$Cos\theta_{bu_i-bu_o} \cong 1 \quad (25)$$

2 Magnitudes of all bus voltages are assumed as equal to 1.0 [p.u.].

3 Transmission line reactances are greater than line resistances; therefore, line resistances can be neglected. Furthermore, if l is the line which connects the input bus bu_i with the output bus bu_o, transmission line reactances and resistences are estimated as follows:

$$g_{bu_i bu_o} = \frac{r_{bu_i bu_o}}{r^2_{bu_i-bu_o} + x^2_{bu_i-bu_o}} = \frac{r_l}{r_l^2 + x_l^2} \approx 0 \quad (26)$$

$$b_{bu_i bu_o} = \frac{x_{bu_i bu_o}}{r^2_{bu_i-bu_o} + x^2_{bu_i-bu_o}} = \frac{x_l}{r_l^2 + x_l^2} \approx -\frac{x_l}{x_l^2} \approx -\frac{1}{x_l} \quad (27)$$

The real power flow balance for each bus of the system is computed in Eq. (28). This equation imposes that the sum of the generated power by all units ($p_{i,\,bu,\,t}$), in addition to the difference between the sum of transmitted power which is entering the bus bu ($p\_l_{l,bu_i,bu_o=bu,t}$) and the sum of transmitted power which is leaving the bus bu ($p\_l_{l,bu_i=bu,bu_o,t}$), are equal to the sum the sum of all power loads.

In this equation, variables $p\_l_{l,bu_i,bu_o,t}$ are replaced by the expression in Eq. (22), but applying the three previous assumptions. Hence, $Cos\theta_{bu_i-bu_o,t}$ is roughly equivalent to $\theta_{bu_i-bu_o}$, and $Sin\theta_{bu_i-bu_o,t}$ is approximately equal to 1 (see Eqs. (24) and (25)). In addition, voltages V_{bu_i} and V_{bu_o} are computed as 1 p.u. Finally, $g_{bu_i bu_o}$ is considered equal to 0 and $b_{bu_i bu_o}$ is assumed as $-\frac{1}{x_l}$, considering that line l connects buses bu_i and bu_o (see Eq. (27)).

$$\sum_{i=1}^{I} p_{i,bu,t} + \sum_{l=1}^{L} p\_l_{l,bu_i,bu_o=bu,t} - \sum_{l=1}^{L} p\_l_{l,bu_i=bu,bu_o,t}$$
$$= \sum_{i=1}^{I} p_{i,bu,t} + \sum_{l=1}^{L}\left(\frac{\theta_{bu_i=bu,t} - \theta_{bu_o=bu,t}}{x_l}\right)$$
$$- \sum_{l=1}^{L}\left(\frac{\theta_{bu_o=bu,t} - \theta_{bu_i=bu,t}}{x_l}\right) = \sum_{c=1}^{C} bkt_{c,bu,t}$$
$$t = 1, \ldots, T \quad (28)$$

The following sign convention is adopted: a power flow entering the bus is assumed positive and a power flow leaving the bus is assumed negative.

3.2. Implementation of binary variables for modeling the line status in the SCUC problem

In the formulation of Eq. (28), line power flows are determined by the differences between the voltage angles of input and output buses. Therefore, the differences between the voltage angles of all connected buses are always computed, even when there are not power flows in transmission lines.

In this work, a more efficient and accurate modeling of the transmission constraints is proposed. For this purpose, a new set of binary variables is incorporated ($y_{l,t}$) for representing the status of the lines. In this model, if the power flow $p\_l_{l,t}$ circulates through the transmission line l at time t, the status of the line is active. In this case, the value of $y_{l,t}$ is 1.

On the other hand, when no power flow circulates through the line l at time t, the line status is inactive and the value of variable $y_{l,t}$ is equal to 0.

$$y_{l,t} = \begin{cases} 1 & if\ p\_l_{l,t} \neq 0 \\ 0 & if\ p\_l_{l,t} = 0 \end{cases} \tag{29}$$

The modeling of transmission constraints with the possibility to active or deactivate lines is presented in the following equations. The calculation of the value of power flow with binary variables is introduced in (30) and (31). M is a large positive constant.

$$\left(\theta_{bu_i,t} - \theta_{bu_o,t}\right) - p\_l_{l,t}x_l \leq \left(1 - y_{l,t}\right)M \quad t = 1, \ldots, T; bu = 1, \ldots, BU; l = 1, \ldots, L \tag{30}$$

$$p\_l_{l,t}x_l - \left(\theta_{bu_i,t} - \theta_{bu_o,t}\right) \leq \left(1 - y_{l,t}\right)M \quad t = 1, \ldots, T; bu = 1, \ldots, BU; l = 1, \ldots, L \tag{31}$$

Constraints (32) and (33) impose the limits for the line power flows:

$$p\_l_{l,t} \leq y_{l,t}\overline{F_l}, \quad t = 1, \ldots, T; l = 1, \ldots, L \tag{32}$$

$$p\_l_{l,t} \geq -y_{l,t}\overline{F_l}, \quad t = 1, \ldots, T; l = 1, \ldots, L \tag{33}$$

Eqs. (34) and (35) show the particular case of constraints (30) and (31) when the status of line l is active (and in accordance, the value of $y_{l,\,t}$ is 1). These equations are used to compute the power flow in line l as the voltage angle difference between buses connected by l, divided by the line reactance.

$$\frac{\left(\theta_{bu_i,t} - \theta_{bu_o,t}\right)}{x_l} \leq p\_l_{l,t} \quad t = 1, \ldots, T; bu = 1, \ldots, BU; l = 1, \ldots, L \tag{34}$$

$$p\_l_{l,t} \leq \frac{\left(\theta_{bu_i,t} - \theta_{bu_o,t}\right)}{x_l} \quad t = 1, \ldots, T; bu = 1, \ldots, BU; l = 1, \ldots, L \tag{35}$$

Otherwise, when the status of line l is inactive (and the value of $y_{l,\,t}$ is 0), Eqs. (30) and (31) are applied as it is showed in constraints (36) and (37). Therefore, in this cases, Eqs. (30) and (31) have no influence over the variables involved, since M is a very large positive constant.

$$\left(\theta_{bu_i,t} - \theta_{bu_o,t}\right) - p\_l_{l,t}x_l \leq M \quad t = 1, \ldots, T; bu = 1, \ldots, BU; l = 1, \ldots, L \tag{36}$$

$$p\_l_{l,t}x_l - \left(\theta_{bu_i,t} - \theta_{bu_o,t}\right) \leq M \quad t = 1, \ldots, T; bu = 1, \ldots, BU; l = 1, \ldots, L \tag{37}$$

The main advantage of incorporating binary variables to a transmission constraint model is the reduction in the number of buses that are dependent on each other. In fact, the classical DC power flow model considers that the voltage angle of bus Θ depends on all buses which are connected to it, even all those buses with no power flow on the connecting line. In contrast, with the proposed model the voltage angle of each bus is computed taking into account only the buses connected to it whose connecting lines are active. Due to this reduction in the interdependence of buses, voltage angles can take other values producing a better distribution of power flows through transmission lines. With the introduction of y-variables in this model that solves a minimization problem, the goal is to increase power flows in some lines by increasing the amount of lines in off-status. The increase is due to the novel model seeks to obtain the smallest possible quantity of variables $y_{l,\,t}$ with value 1. If there are fewer active lines, variables Θ have fewer active restrictions. Consequently, by applying the proposed model, alternative solutions with lower costs can be found, that are not provided by classical models.

Additionally, the implementation of the binary variables for the active/inactive status of each line may facilitate the maintenance of power systems, since the scheduling obtained allows to identify lines at inactive status that can be taken out of service.

3.3. An illustrative example

With the aim of illustrating the scope of the incorporation of binary variables for modeling the transmission network and the advantages of the proposed model, two simple cases are presented in Fig. 1. The one-line diagram of this figure corresponds to a power system with four buses, four transmission lines, one unit located at the bus 1, and one load located at the bus 4. In this system, transmission losses are neglected. The power produced by the unit is 60 [MW], and it must be transmitted from the bus 1 to the bus 4 where the load is located.

In Case A, transmission constraints are modeled using the classical DC power flow model. In this case, a power flow of 28.421 [MW] circulates trough lines 1 and 3, and a power flow of 31.579 [MW] circulates trough lines 2 and 4. As a consequence, the value of the voltage angle of bus 1 (Θ_1) depends on relationships between buses 1-2 via Eq. (38), and buses 1-3 through Eq. (39).

$$p\_l_1 = \frac{\theta_1 - \theta_2}{x_1} = 28.421[MW] \tag{38}$$

$$p\_l_2 = \frac{\theta_1 - \theta_3}{x_2} = 31.579[MW] \tag{39}$$

In Case B, y-binary variables are implemented to model transmission constraints. In this case, a power flow of 60 [MW] circulates from the bus 1 to the bus 4, through lines 1 and 3. The power flows in line 1 and 3 are modeled by constraints (30–33). The status of these lines is active and thus the values of y_1 and y_3 are 1. These constraints ensure that the power flows on the lines 1 and 3 are limited by their maximum capacities.

However, in Case B there is no power flows on lines 2 and 4, thus these lines are inactive and the values of y_2 and y_4 are 0. With these values, constraints (30–33) are deactivated, i.e., they have no influence over the variables involved.

In Case A, variable Θ_1 depends on two relationships with Θ_1-Θ_2 and Θ_1-Θ_3, since there are power flows on lines 1 and 3. Instead, in Case B, variable Θ_1 depends only on the relationship with Θ_2 because lines 2 and 4 are inactive. Indeed, for the solution obtained with the proposed model, power flows on lines 1 and 3 are increased, enabling lines 2 and 4 to be deactivated.

This simple example illustrates the fact that the proposed model, including y-binary variable can represent more solutions

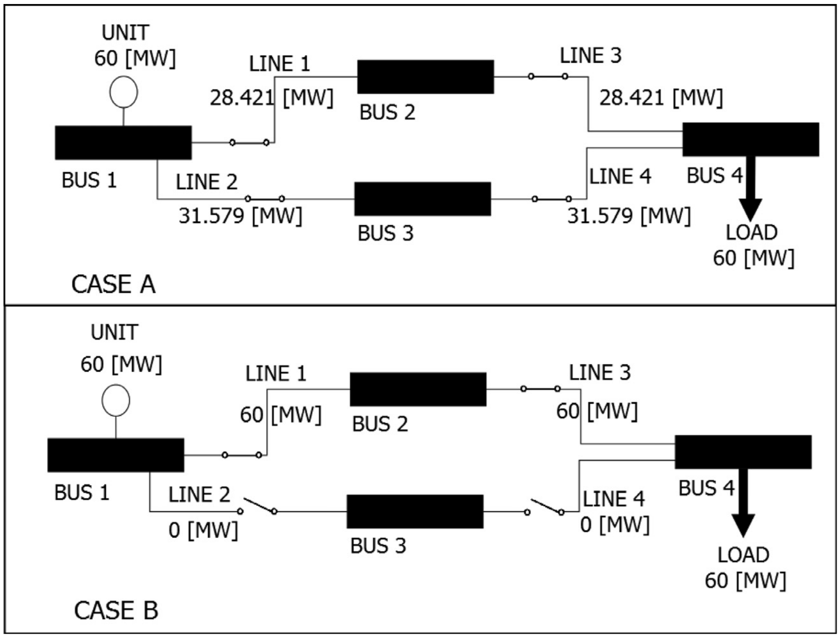

Fig. 1. Illustrative example. One-line diagram: Cases A and B.

than the classical model. For this example, both solutions can be obtained with the novel model, while the optimization process chose the solution of case B as the best option for operating the system when the proposed model is solved. However, the solution of case B is infeasible for the classical DC model; in fact, there is not a possible combination of the voltage angles between buses 1-2/1-3 and 2-4/3-4 in order to lines take values of 60 or 0 [MW], respectively. Then, for the example illustrated, none of the aforementioned relationships can be deactivated with the classical model.

Releasing lines in certain periods of time allow maintenance and other activities without affecting the supply of demand.

4. Numerical test

The proposed model was implemented for three power systems in General Algebraic Modeling System (GAMS). Solvers CPLEX and Gurobi were applied in an Intel i5 (2.67 Ghz), 4 GB Ram computer.

First, a 6-bus power system is solved in order to illustrate the methodology. Second, a 31-bus power system is addressed, and for this case, results are analyzed and interpreted graphically. Finally, to prove the effectiveness of the proposed model the well-known IEEE 118-bus power system is studied. This last power system is about 18 times larger than the first system and 4 times larger than the second one.

4.1. 6-bus system

First, a 6-bus system was addressed. The data for this system can be found in (Grey & Sekar, 2008). This system consists of 3 generators, 3 loads, and 11 transmission lines. Fig. 2 shows the corresponding one-line diagram. Three cases of this system were tested to show the importance of considering transmission constraints and the effects of including binary variables for their modeling.

Case 4.1.1: Firstly, the UC problem without network constraints is considered. Operational costs of this system and CPU times for the optimal solutions obtained with solvers CPLEX and Gurobi are shown in Table 1. The solutions obtained with these solvers present the same objective value $ 73,721 and very similar execution times. The solution of this case is $4601 lower than the solution reported in (Grey & Sekar, 2008).

Table 1
6-bus system, Case 4.1.1: UC Problem. Performance of solvers.

Solver	Cost [$]	CPU time [s]
CPLEX	73721.7	0.110
Gurobi	73721.7	0.104

The absolute gap is the difference between the objective value of the best known solution and the best lower bound of the objective function, and the relative gap is the absolute gap divided by the best lower bound. In this case, the relative gap was set at 0.

Table 2 shows the schedule of commitments, where 1/0 represent the ON/OFF status of each unit for each time period during the programming horizon. Unit 1 is ON during the entire programming horizon while units 2 and 3 are used at peak periods to reach the demand.

The model is composed of 1196 equations, 289 continuous variables and 72 binary variables.

Case 4.1.2: In the second case UC problem with transmission constraints is solved, by implementing the classical model, i.e. the problem known as SCUC problem. In order to illustrate the effects of network constraints on the total cost, the data for transmission lines were modified in this case. Table A1 in Appendix A shows the new limits for power flow lines.

If the solution obtained in the previous case for UC problem is applied to this model, it results to be infeasible since the values for power outputs obtained from UC schedule cannot adjust the limitations of the lines.

Table 3 shows the values of objective functions and CPU times obtained with solvers CPLEX and Gurobi when the relative gap 0 is required.

After including transmission constraints, the optimal total cost resulted around 5.5% higher than the one obtained for the UC problem. Table 4 shows the schedule of commitments in this instance.

Transmission line power flows for each time period are shown in Table 5. The negative values of power flows indicate that the

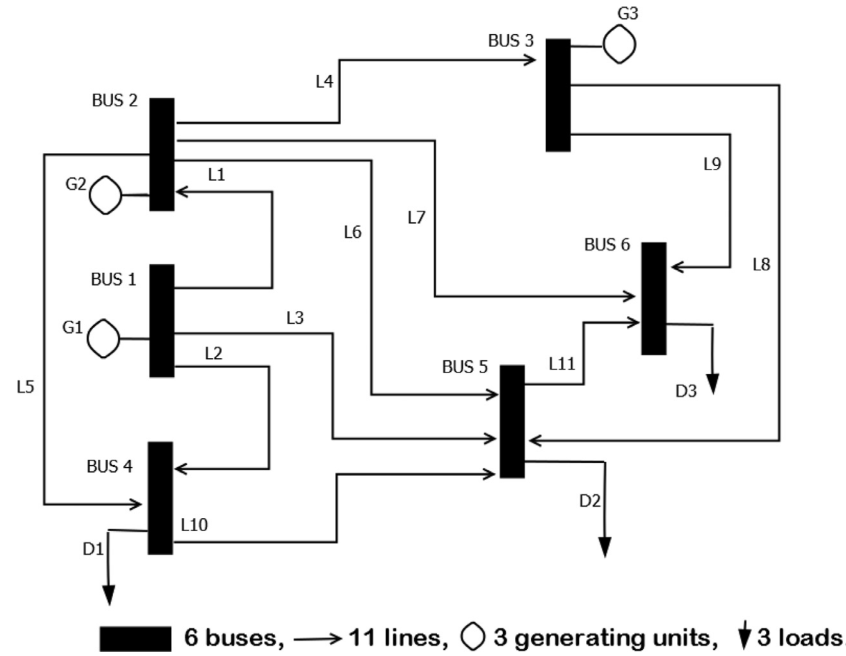

Fig. 2. 6- bus system: one-line diagram.

Table 2
6-bus system, Case 4.1.1: UC Problem. Schedule of committed units.

	HOURS																							
U	1	2	3	4	5	6	7	8	9	10	11	12	13	14	15	16	17	18	19	20	21	22	23	24
G1	1	1	1	1	1	1	1	1	1	1	1	1	1	1	1	1	1	1	1	1	1	1	1	1
G2	0	0	0	0	0	0	0	0	0	0	0	0	0	0	0	0	0	1	1	1	0	0	0	0
G3	0	0	1	0	0	0	0	0	0	1	1	1	1	1	1	1	1	0	0	0	1	1	1	0

Table 3
6-bus system, Case 4.1.2: SCUC Problem with classical DC model. Performance of solvers.

Solver	Cost [$]	CPU time [s]
CPLEX	77775.1	0.249
Gurobi	77775.1	0.149

directions of these flows are inverse to the ones originally assumed (see Fig. 2). The table also shows that there are four time periods (hours 18–21) in which some of the lines 4, 6, 8, 10, or 11 are inactive.

In this case, the SCUC model with DC transmission constraints includes 2396 equations, 2017 continuous variables and 72 binary variables.

Case 4.1.3: For the third case, SCUC problem is solved, including $y_{l,t}$ binary variables for modeling transmission constraints. The production costs and CPU times obtained with both solvers by requiring relative gap 0 are shown in Table 6. Similar to case 4.1.1, the optimal cost is 5.0% higher than the one obtained for the UC problem in case 4.1.1. However, the incorporation of binary variables for modeling transmission constraints enables alternative solutions that cannot be represented through the classical model. As a result, the optimal cost obtained in this case is slightly lower than the one obtained with the classical model in case 4.1.2.

Table 7 presents the schedule of commitments. As in previous cases, unit 1 is ON at all time periods. Unit 2 is committed at hours 10–17 and 20–23, and unit 3 is committed only at hours 18–20.

Transmission line scheduling for this case is shown in Table 8. This table shows that there are 19 time periods (hours 1–10, 14–16, 18–21, and 23–24) in which some of the lines 4, 6, 8, 10, or 11 have no power flows. This number of periods in which some lines are inactive is considerably higher than the one obtained with the classical model in case 4.1.2. Thus, another important advantage of the proposed model is the fact it allows to obtain a higher number of lines and hours available for receiving maintenance.

This model consists of 2396 equations, 2017 continuous variables, and 336 binary variables.

Table 4
6-bus system, Case 4.1.2: SCUC Problem with classical DC model. Schedule of committed units.

	Hours																							
Unit	1	2	3	4	5	6	7	8	9	10	11	12	13	14	15	16	17	18	19	20	21	22	23	24
G1	1	1	1	1	1	1	1	1	1	1	1	1	1	1	1	1	1	1	1	1	1	1	1	1
G2	0	0	0	0	0	0	0	0	0	1	1	1	1	1	1	1	1	0	0	1	1	1	1	0
G3	0	0	0	0	0	0	0	0	0	0	0	0	0	0	0	0	0	1	1	1	1	0	0	0

Table 5
6-bus system, Case 4.1.2: SCUC Problem with classical DC model. Transmission line scheduling, in MW.

Hour	Transmission Line										
	L1	L2	L3	L4	L5	L6	L7	L8	L9	L10	L11
1	73.97	91.99	55.14	10.98	36.03	5.82	21.14	−3.80	14.82	−4.60	8.27
2	68.25	84.87	50.87	10.13	33.25	5.37	19.50	−3.50	13.67	−4.30	7.63
3	64.47	80.17	48.06	9.57	31.40	5.08	18.42	−3.30	12.92	−4.00	7.20
4	62.56	77.80	46.64	9.29	30.47	4.93	17.88	−3.20	12.53	−3.90	6.99
5	60.69	75.47	45.24	9.01	29.56	4.78	17.34	−3.10	12.16	−3.80	6.78
6	61.63	76.64	45.94	9.15	30.02	4.85	17.61	−3.20	12.35	−3.90	6.89
7	62.56	77.80	46.64	9.29	30.47	4.93	17.88	−3.20	12.53	−3.90	6.99
8	67.35	82.83	48.22	10.83	30.95	3.31	22.25	−6.60	17.43	−5.30	0.00
9	75.85	94.32	56.54	11.26	36.94	5.97	21.67	−3.90	15.19	−4.80	8.48
10	74.03	97.46	57.91	13.48	46.87	8.56	25.12	−3.10	16.56	−5.30	8.19
11	75.94	99.84	59.33	13.76	47.80	8.71	25.67	−3.20	16.94	−5.40	8.41
12	75.38	100	59.35	14.07	49.25	9.09	26.14	−3.00	17.11	−5.50	8.33
13	75.94	99.84	59.33	13.76	47.80	8.71	25.67	−3.20	16.94	−5.40	8.41
14	74.03	97.46	57.91	13.48	46.87	8.56	25.12	−3.10	16.56	−5.30	8.19
15	73.01	96.16	57.16	13.34	46.31	8.49	24.86	−3.00	16.37	−5.20	8.09
16	73.01	96.16	57.16	13.34	46.31	8.49	24.86	−3.00	16.37	−5.20	8.09
17	75.38	100	59.35	14.07	49.25	9.09	26.14	−3.00	17.11	−5.50	8.33
18	70.23	100	52.68	0	59.55	0	10.68	15.76	44.74	−10.50	1.26
19	70.99	100	59.67	−2.80	58.01	0	15.80	0	38.62	−5.20	0
20	71.99	100	59.34	13.34	56.02	0	29.06	0	24.78	−5.50	0
21	70.08	100	55.96	14.45	59.84	9.24	26.90	−3.20	17.68	0	8.69
22	74.57	100	59.25	14.41	50.86	9.54	26.65	−2.90	17.27	−5.60	8.23
23	73.09	96.30	57.21	13.34	46.42	8.48	24.86	−3.00	16.37	−5.20	8.09
24	76.82	95.52	57.26	11.40	37.42	6.05	21.95	−4.00	15.39	−4.80	8.58

Table 6
6-bus system, Case 4.1.3: SCUC Problem including y binary variables. Performance of solvers.

Solver	Cost [$]	CPU time [s]
CPLEX	77423.6	2.496
Gurobi	77423.6	2.711

4.2. 31- bus system

This system has 31 buses, 16 generating units and 43 lines. The data for this system can be found in (Guo, 2012) and its one-line diagram is depicted in Fig. 3. Here again, three cases are considered: the UC problem, the SCUC problem with classic DC power flow model, and finally, the SCUC problem with the proposed y binary variables ($y_{l,t}$).

Case 4.2.1: In this case, the UC problem without network constraints is considered. Table 9 presents the optimal costs and computational times obtained with solvers CPLEX and Gurobi, requiring relative gap 0. Gurobi resulted almost 8 s faster than CPLEX. The model includes 7307 equations, 1537 continuous variables, and 384 binary variables.

Case 4.2.2: In this case, SCUC problem is considered by implementing the classical DC power flow. The optimal operation costs and CPU times are presented in Table 10**.** Due to the application of transmission constraints, the operating cost obtained in this case with both solvers is $ 2173 higher than the optimal cost of the UC problem in case 4.2.1. To reach relative gap 0, solver Gurobi required 18.2 s less than CPLEX. The model in this case is composed of 12,179 equations, 8473 continuous variables, and 384 binary variables.

Case 4.2.3: Finally, SCUC problem with the proposed $y_{l,t}$ binary variables for modeling transmission constraints is considered. The model in this case is composed of 12,179 equations, 8473 continuous variables, and 1416 binary variables. Logically, the model has more variables than the previous case. Consequently, this model resulted harder to solve by requiring relative gap 0. Then, different CPU time limits were tested with the aim of analyzing the performance of the model; Table 11 shows the results. For each CPU time limit, total costs and relative gaps for both solvers are very close. Considering the cases tested, it can be seen that increasing the time limit does not necessarily lead to better solutions. In fact, cost savings for high time limits are minor. Solvers can find good solutions easily, but they spend too much time trying to reduce the gap. Then, it can be concluded that optimal solutions for the proposed model can be found in relative short CPU time, reaching tight relative gap, even though relative gap 0 is not warranted.

On the other hand, for time limits greater than 200 s, the optimal costs obtained with the proposed model are lower than the ones obtained in case 4.2.2 with the classic DC power flow model. As was mentioned before, real alternative solutions can be represented when $y_{l,t}$ binary variables are incorporated for transmission modeling, that are unfeasible for the classic DC power flow model. Thus, this case exemplifies that cost savings can be achieved with the proposed model since solutions with better operating cost can be obtained.

Regarding lines that are inactive in some period of time, for example the solution obtained with CPLEX and 10,000 s of time limit presents a total of 261 time periods in which some line is

Table 7
6-bus system, Case 4.1.3: SCUC Problem including y binary variables. Schedule of committed units.

	Hours																							
Unit	1	2	3	4	5	6	7	8	9	10	11	12	13	14	15	16	17	18	19	20	21	22	23	24
G1	1	1	1	1	1	1	1	1	1	1	1	1	1	1	1	1	1	1	1	1	1	1	1	1
G2	0	0	0	0	0	0	0	0	0	1	1	1	1	1	1	1	1	0	0	1	1	1	1	0
G3	0	0	0	0	0	0	0	0	0	0	0	0	0	0	0	0	0	1	1	1	0	0	0	0

Table 8
6-bus system, Case 4.1.3: SCUC Problem including y binary variables. Transmission line scheduling, in MW.

Hour	Transmission Line										
	L1	L2	L3	L4	L5	L6	L7	L8	L9	L10	L11
1	74.11	92.03	54.96	12.84	35.83	0	25.44	−5.9	18.78	−4.8	0
2	68.03	86.15	49.82	11.56	36.25	0	20.22	0	11.56	0	9.01
3	61.7	79.67	51.33	0	35.95	0	25.75	−5.8	5.81	0	6.97
4	61.54	78.43	47.03	0	33.77	5.99	21.78	−7.1	7.10	0	8.52
5	58.08	75	48.32	0	33.84	0	24.24	−5.5	5.47	0	6.56
6	58.98	76.16	49.06	0	34.36	0	24.62	−5.6	5.55	0	6.66
7	61.94	77.62	47.44	11.12	31.36	0	19.46	0	11.12	−3.2	6.82
8	65.71	82.35	50.34	11.8	33.27	0	20.65	0	11.8	−3.4	7.23
9	74.79	95.2	56.71	11.74	40.82	0	22.24	−3.4	15.13	0	7.97
10	72.43	98.16	58.81	14.55	51.48	0	26.4	−1.9	16.41	0	7.07
11	75.94	99.84	59.33	13.76	47.8	8.70	25.67	−3.2	16.94	−5.4	8.40
12	75.38	100	59.35	14.07	49.25	9.09	26.14	−3	17.11	−5.5	8.33
13	75.94	99.84	59.33	13.76	47.8	8.70	25.67	−3.2	16.94	−5.4	8.40
14	74.02	99.22	56.16	14.71	50.42	0	28.89	−6.3	20.99	0	0
15	71.41	96.84	58.08	14.42	50.85	0	26.14	−1.8	16.22	0	6.96
16	71.41	96.84	58.08	14.42	50.85	0	26.14	−1.8	16.22	0	6.96
17	75.38	100	59.35	14.07	49.25	9.09	26.14	−3	17.11	−5.5	8.33
18	70.23	100	52.68	0	59.55	0	10.68	15.76	44.74	−10.5	1.25
19	70.99	100	59.67	−2.8	58.01	0	15.8	0	38.62	−5.2	0
20	71.99	100	59.34	13.34	56.02	0	29.06	0	24.78	−5.5	0
21	70.08	100	55.96	14.45	59.84	9.24	26.9	−3.2	17.68	0	8.69
22	74.57	100	59.25	14.41	50.86	9.53	26.65	−2.9	17.27	−5.6	8.22
23	73.07	98.03	55.5	14.57	49.93	0	28.58	−6.2	20.74	0	0
24	77.56	97.63	54.41	12.07	40.13	0	25.36	−8.5	20.56	0	0

Table 9
31- bus system, Case 4.2.1: UC Problem. Performance of solvers.

Solver	cost [$]	CPU time [s]
CPLEX	1103044.7	62.7
Gurobi	1103044.7	50.9

Table 10
31-bus system, Case 4.2.2: SCUC with classical DC model. Performance of solvers.

Solver	Cost [$]	CPU time [s]
CPLEX	1105217.9	122.7
Gurobi	1105217.9	104.5

Table 11
31- bus system, Case 4.2.3: SCUC with y binary variables. Performance of solvers.

Solver	COST [$]	REL. gap	CPU t. limit [s]
CPLEX	1125110.1	0.0236	100
Gurobi	1105484.6	0.0027	100
CPLEX	1105741.1	0.0023	500
Gurobi	1104987.0	0.0012	500
CPLEX	1105668.3	0.0019	1000
Gurobi	1104962.6	0.0010	1000
CPLEX	1105554.3	0.0016	3600
Gurobi	1104702.2	0.0007	3600
CPLEX	1104538.4	0.0006	10,000
Gurobi	1104581.8	0.0004	10,000

inactive. This constitutes an increase of 522% with respect to this amount for the solution obtained with the classical DC model in case 4.2.2. In these time periods, inactive lines may receive maintenance, among other applications.

4.3. IEEE 118- bus system

The well-known IEEE 118-bus system (Badakhshan, Kazemi, & Ehsan, 2015; Lotfjou, Shahidehpour, & Fu, 2010; Reza Norouzi et al., 2014), is implemented to study the performance of binary variables $y_{l,t}$. The system has 54 thermal units, 186 transmission lines, and 91 loads. The one-line diagram is shown in Fig. 4 and the data for this system can be found in **Appendix B**. Here again, three cases were solved.

Case 4.3.1: the base UC problem without transmission constraints was solved. Table 12 presents the optimal costs and CPU times for solvers tested when relative gap 0 is required. For this case, both solvers have very similar performances. The model has 26,389 equations, 5185 continuous variables, and 1296 binary variables.

Case 4.3.2: In the second case, transmission constraints modeled with the classical DC power flow model are considered. Table 13 shows that the optimal operating cost increases $8,946,199 respect to the UC problem. CPLEX is 44 s faster than Gurobi, when the relative GAP is set to zero. The size of this model is: 47,077 equations, 34,801 continuous variables, and 1296 binary variables. In this case, there are only 17 time periods in which some lines are inactive.

Case 4.3.3: In this case, binary variables $y_{l,t}$ are applied to model transmission constraints in the SCUC problem. By applying the proposed model, a cost saving of up to 3.6% is achieved. The model of this case is composed of 47,077 equations, 34,801 continuous variables, and 5760 binary variables. Here again, due to the higher number of binary variables, the model is hard to solve by requiring relative gap 0. Then, five different time limits were tested for this case.

Table 12
IEEE 118-bus system, Case 4.3.1: UC Problem. Performance of CPLEX and Gurobi.

Solver	Cost [$]	CPU time [s]
CPLEX	133,983,648	3.8
Gurobi	133,983,648	3.5

Table 13
IEEE 118-bus system, Case 4.3.1: SCUC problem with classical DC model. Performance of CPLEX and Gurobi.

Solver	Cost [$]	CPU time [s]
CPLEX	142,947,848	37.2
Gurobi	142,947,848	81.4

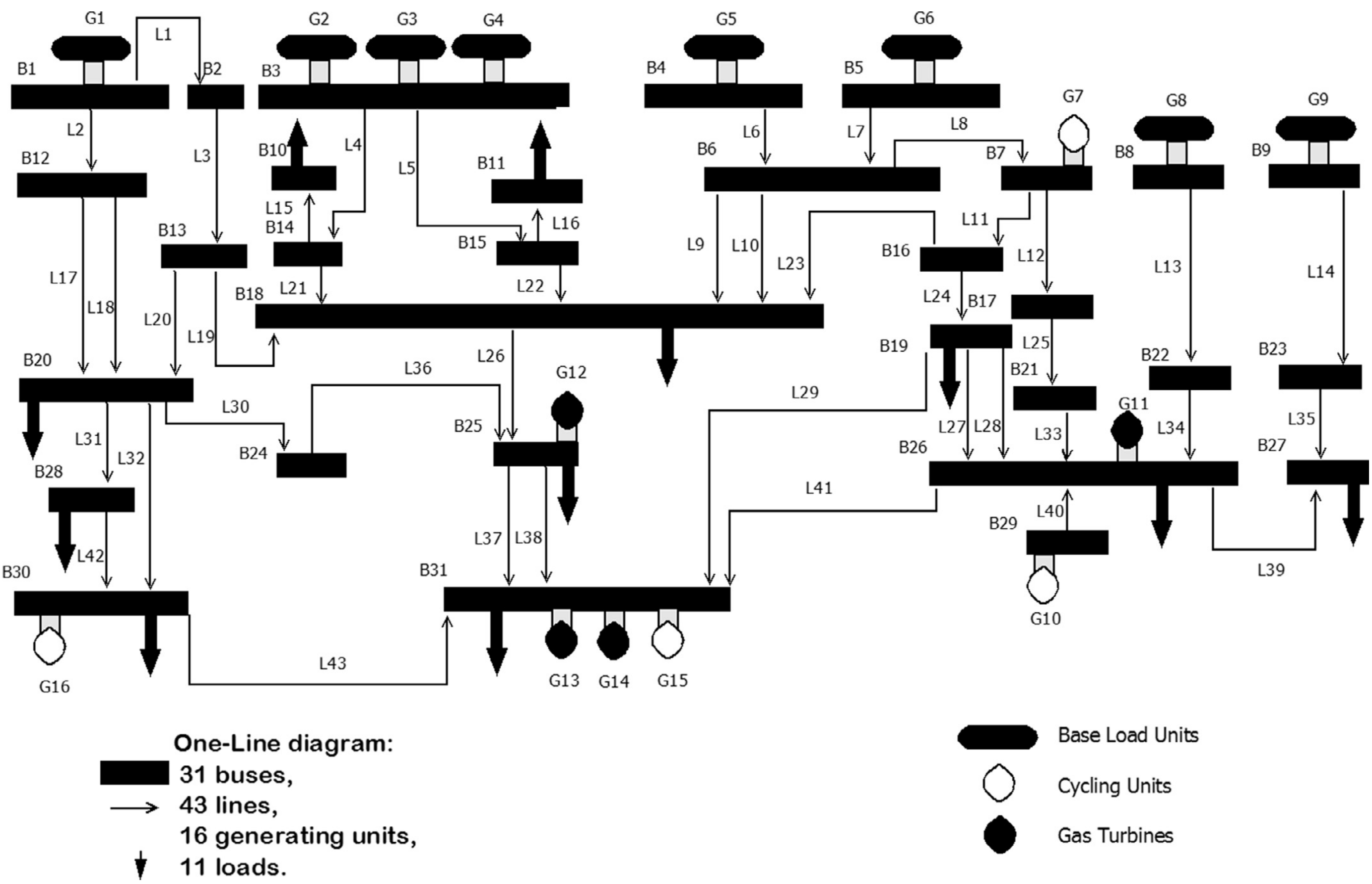

Fig. 3. 31-bus system: one-line diagram.

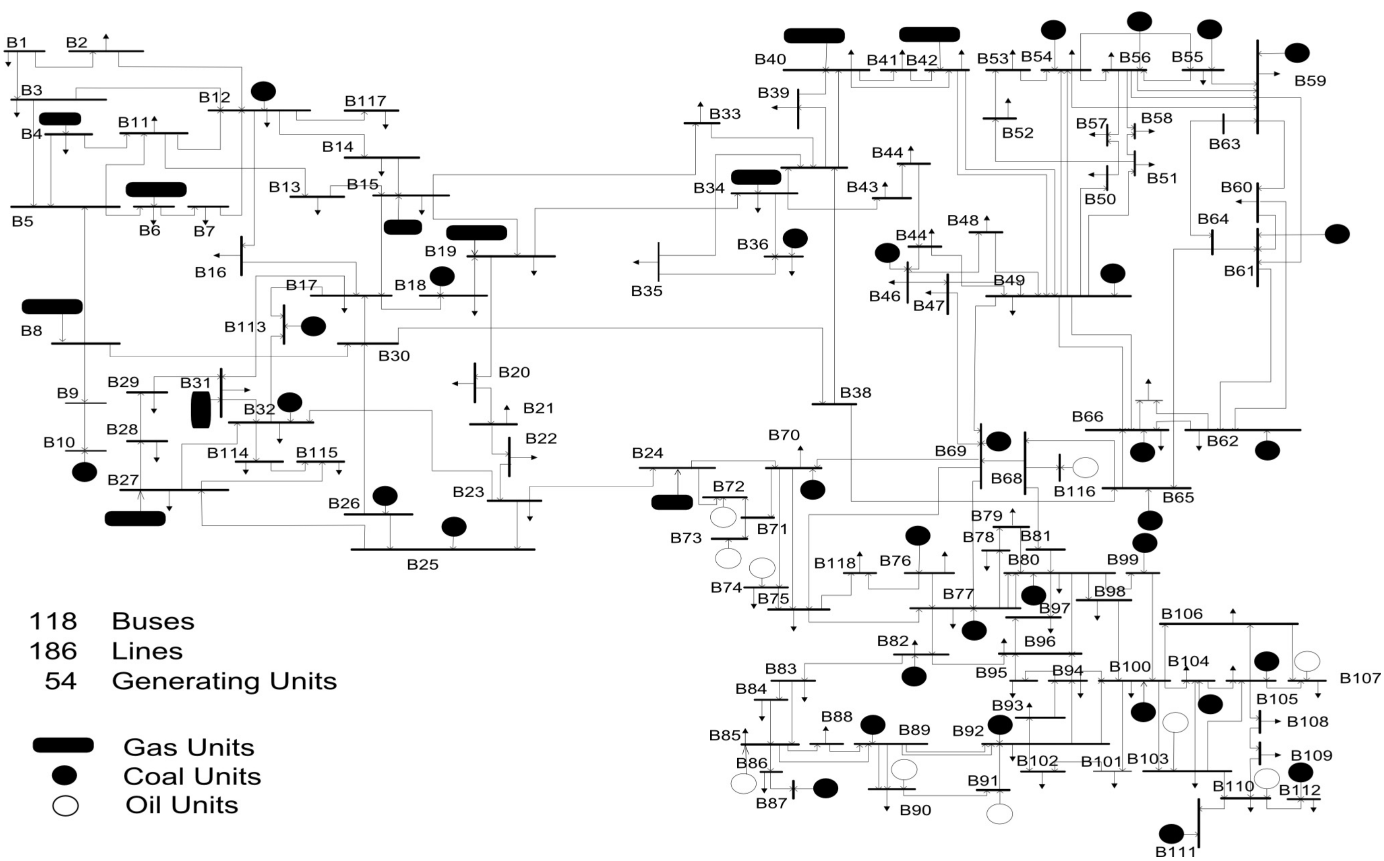

Fig. 4. IEEE 118-bus system: one-line diagram (Illinois Center for a Smarter Electric Grid, 2013).

Table 14
IEEE 118-bus system, Case 4.3.1: SCUC problem with classical DC model. Performance of solvers.

Solver	Cost [$]	REL. gap	CPU t. limit [s]
CPLEX	151612810.9	0.1145	100
Gurobi	No solution returned	–	100
CPLEX	141177337.6	0.0490	500
Gurobi	No solution returned	–	500
CPLEX	140017162.3	0.0406	1000
Gurobi	No solution returned	–	1000
CPLEX	137753403.3	0.0248	3600
Gurobi	137977523.4	0.0256	3600
CPLEX	135976766.5	0.0119	10,000
Gurobi	137015247.2	0.0185	10,000

Performances for both solvers are presented in Table 14. For CPU time limits up to 1000 s, Gurobi is unable to obtain a feasible solution. For this case CPLEX exhibits a better performance, finding good solutions in few seconds, and improving it when the time limit increases. For CPU time limits higher than 500 s, the solutions obtained with CPLEX present costs considerably lower than the optimal solutions obtained with the classic DC power flow model in case 4.3.2. In fact, at 1000 s, the cost of the solution obtained with CPLEX is $2,930,686 lower than the one obtained in case 4.2.3; at 3600 s, the cost saving is $5,194,445, while at 10,000 s of the CPU time limit, the solution obtained with the proposed model is $6,971,082 lower than the one for the classical DC model.

This example also illustrates that the proposed model is capable of representing more solutions than the classical model, and in this way it is possible to find solutions more economic that satisfy the required demand.

For the systems previously tested, the performances of Gurobi are better than CPLEX. But, in this case, CPLEX reaches feasible solutions with lower operating costs than Gurobi for all CPU time limits.

For the best solution found in this case with the proposed model, there are 947 time periods in which some lines are inactive. This constitutes an increase of 5570% in the number of such time periods compared with the best solution found with the classical model in case 4.3.2.

5. Analysis of results

5.1. 6-bus system

Clearly, the total generating cost obtained for the UC problem is lower than the one obtained for the SCUC problem (with the classical DC model), due to the implementation of transmission constraints. In this case, when transmission line limits are taken into account, the obtained solution implies that the units must generate in a more expensive way, in comparison with the solution of UC problem.

Furthermore, with the proposed model a reduction in the total cost was achieved, compared to the classical DC model, and that is due to the inclusion of $y_{l,t}$ variables. Indeed, a greater number of feasible solutions can be obtained by the application of the novel model. This fact increases the chances of obtaining cheaper solutions. In addition, it increases the number of inactive lines (available to receive maintenance), comparing the DC model and the new model.

5.2. 31-bus system

For the 31-bus system, the situation is similar to 6-bus system. SCUC problem solution is higher than UC solution, as consequence of transmission constraints.

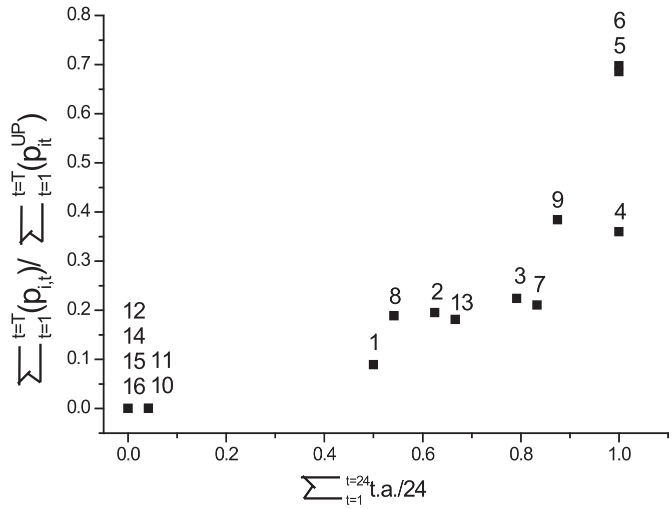

Fig. 5. 31-bus system. Utilization factor versus commitment factor for generating units.

Comparing results of the classical DC model and the new transmission model, it can be seen that there is a decrease in the total cost and the increase of 522% in the number of inactive lines, are due to the qualities of the novel model, which have been detailed above.

The 31-bus power system is chosen for presenting a more detailed analysis of the obtained results through graphics.

The analysis of generator performance is crucial for the system operation; it allows identifying which unit is operating close to its maximum capacity as well as its participation in the total power produced.

Fig. 5 illustrates the relationships between power produced by units and their committed times. Abscissa axis represents the *commitment factor for generating units* (40), which is the sum of hours during which the unit is committed (active time ($t.a._i$)) divided by the programming horizon, usually 24 h are adopted.

$$\frac{\sum_{t=1}^{T} t.a._i}{24}, \in [0, 1] \; i = 1, \; \ldots, I \tag{40}$$

Ordinate axis represents the *utilization factor for generating units*, which is the ratio of the power produced ($p_{i,\,t}$) divided by the maximum power produced by units along the programming horizon ($p_{i,t}^{UP}$) (41).

$$\frac{\sum_{t=1}^{T} p_{i,t}}{\sum_{t=1}^{T} p_{i,t}^{UP}}, \; \in \; [0, 1] \; i = 1, \; \ldots, I \tag{41}$$

Fig. 5 shows that there are three generators occupied 100% of the time horizon: units 6, 5 and 4. Units 10, 11, 12, 14, 15 and 16 have values lower than 10% for both factors; even, four of them are offline along the whole time horizon. For units 1, 2, 3, 7, 9 and 13 both factors assume values between 10% and 90%. Hence, it can be appreciated that units 5-6 present the major contribution to the power system, because they present values of 1 for both factors. Units 9 and 4 also represent a great importance for the system because they have elevated percentages for both factors (over 50%), although they have lower values than units 5-6. It means that these four units are committed the major part of the programming horizon and produce 59.3% of the total power generation.

Transmission lines are also analyzed, since their role in meeting the demand is equally important. The performances of lines with highest incidence in the system are presented in Fig. 6.

Abscissa axis represents the programming horizon. Ordinate axis represents the *utilization factor for transmission line*, which is

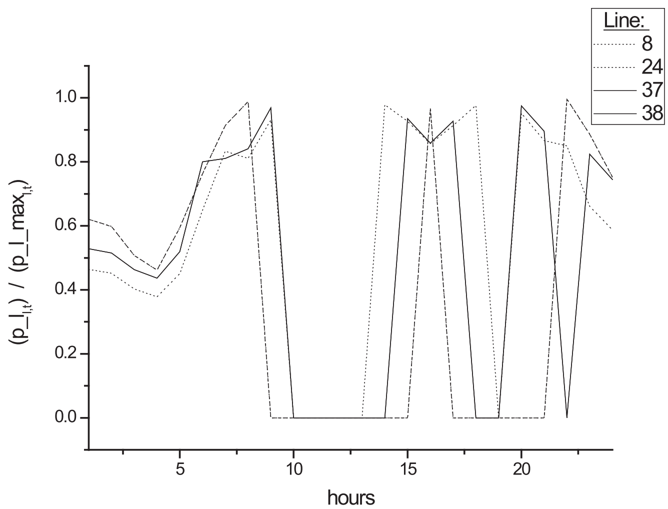

Fig. 6. 31-bus system. Utilization factor for transmission line.

the power flow in line l at time t $(p\_l_{l,t})$, divided the maximum line capacity $(\bar{F}_{l,t})$ (42). The lines illustrated in the figure are the four lines with higher utilization factor for transmission line: lines 8, 24, 37 and 38; besides, lines 37 and 38 assume the same values.

Figure shows that these four lines are very close to their maximum capacities at three time intervals: (1) between hours 7 and 9, (2) between hours 12 and 17, and (3) between hours 19 and 23. Three intervals match with the higher values of the hourly demand.

$$\frac{p\_l_{l,t}}{\bar{F}_{l,t}}, \in [0,1] \; l = 1, \ldots, L; \; t = 1, \ldots, T \tag{42}$$

Fig. 7 displays the one-line diagram for the system, highlighting the lines with highest and lowest utilization factors. It is important to identify lines with highest utilization factors because they are close to their power flow limits. As a consequence, an increase in the demand could overload these lines. Furthermore, it is important to identify which lines have the lowest utilization factors. In this system, there are three lines with low utilization factor: lines 11, 39, and 40. A low value for this factor indicates a waste of valuable resources of the system. For example, in case of an increase in the demand, a possible solution would be to install new generators in buses near to lines with low utilization. This constitutes an option to meet the demand without needing to invest in new lines.

In Fig. 7, four lines with highest utilization factor are highlighted and labeled with HF. Particular attention should be paid to these lines because they are close to their limit. Hence, if any of them is out of service, this could raise problems, in particular, for the connections of buses: lines 37 and 38 connect bus 31 which has a load and three generators. Line 24 is the only connection between buses 19 and 16. In addition, buses 6 and 7 are connected only by line 8.

Three lines with the lowest values of utilization factor are also highlighted and labeled with LF. In the figure, it can be appreciated than lines 11 and 39 are important for the system because are the only connection between buses 7–16 and 26-27, but respectively, the importance of line 40 is greater because it is the only connection between bus 29 and the rest of the power system. If this line is damaged, generator 10 could not transmit its power output.

If losses are considered as negligible, the power flow entering to bus is the same as the output power flow Eq. (22). The following figure helps with the interpretation of power magnitudes that are supported by each bus. Thus, Fig. 8 shows the sum of power flow entering the bus *bu* from generator *i* and line *l* for each time period (43) along the programming horizon. For clarity purposes, only the

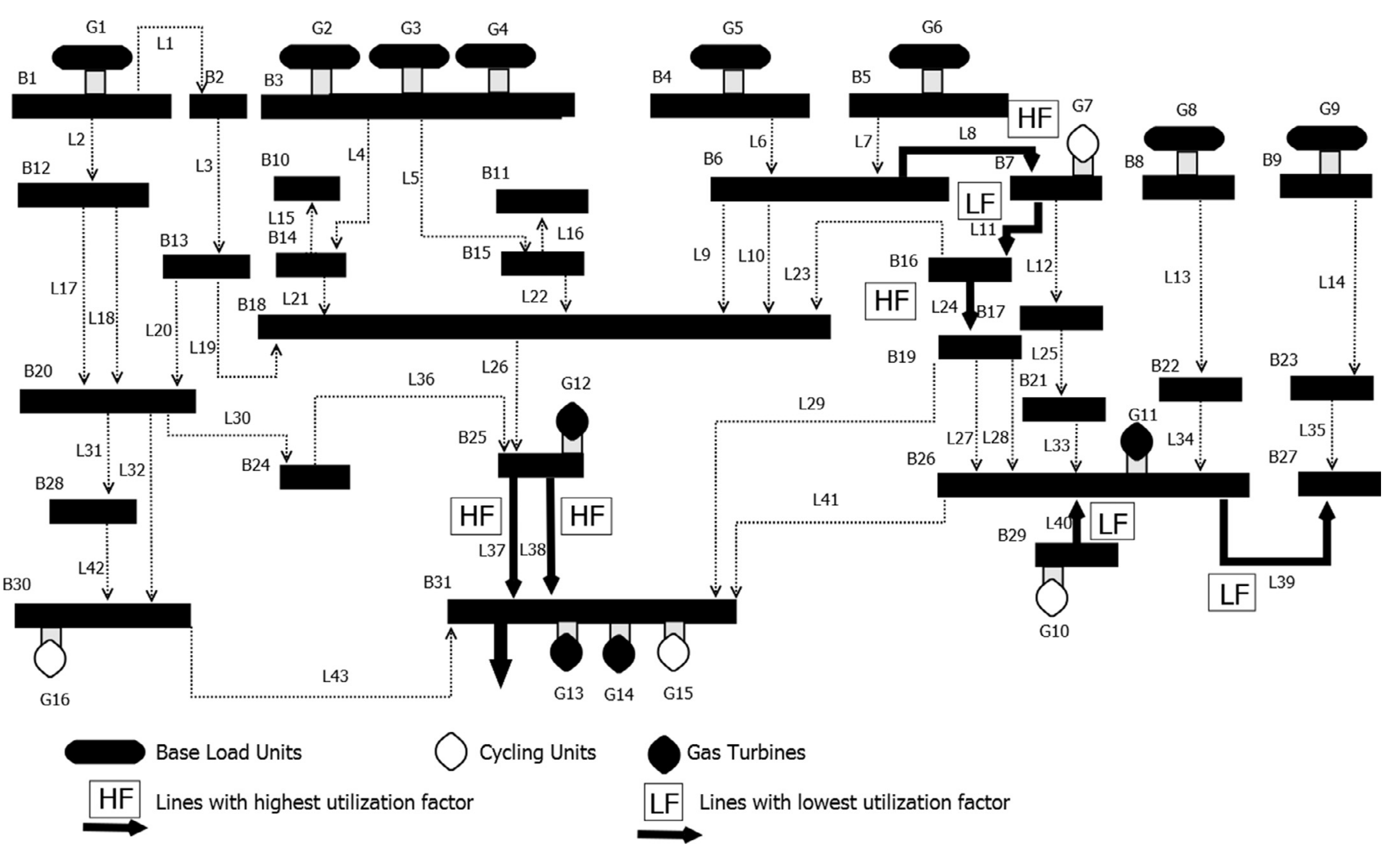

Fig. 7. 31- bus system. Lines with the highest and lowest values of transmission factor.

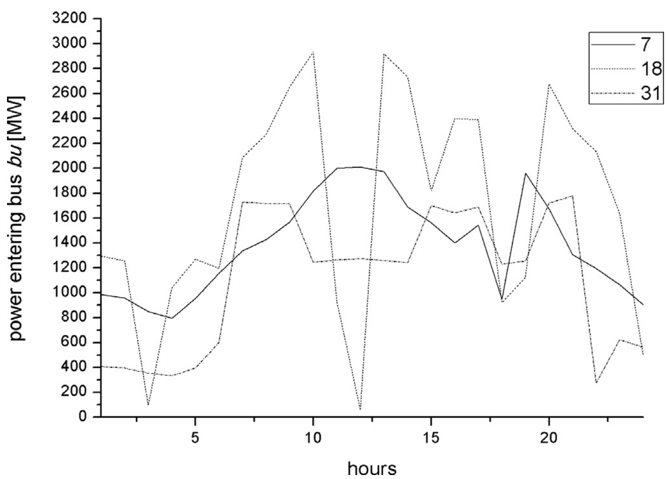

Fig. 8. 31-bus system. The three buses with biggest sums of power flow entering to them.

3 buses with biggest sums of power flow entering are depicted in Fig. 8: buses 7, 18, and 31. These buses must be able to support power flows higher than 2000, 2970, and 1800 [MW], respectively, according to the maximum values of power flow entering buses per hour indicated in the figure.

$$\sum_{i=1}^{I} p_{i,bu_i=bu,t} + \sum_{bu=1}^{BU}\sum_{l=1}^{L} p\_l_{l,bu_i=bu,t,bu_o}\ [MW],\ \ t = 1,\ \ldots, T \qquad (43)$$

It is important to identify these buses that are critical for the power system. In fact, an excess of power flows in one of these buses would cause a technical failure, with serious complications affecting the whole system such as: generators or loads may result isolated.

As can be seen from one-line diagrams, the input bus bu_i is connected to the output bus bu_o through the line l. A graphical representation of relationships between lines and buses is shown in Fig. 9, which depicts the *utilization factor for lines at hours with power flow* at the ordinate axis along the time horizon. This factor is the sum of power flows of line l divided by the sum of maximum power flow which line l can support Eq. (44). The sum is computed over the hours at which power flow circulates through each line. *Line - input/output bus factors* are computed for each line at the two buses the line connects (Eqs. (45) and ((46)); and they are presented in abscissa axis. Eq. (45) represents the *line - input bus factor*, which is computed as the ratio between the sum of power flows which are entering the bus $bu_i = bu$ through line l, and the sum of power flows from all lines which are entering the common bus $bu_i = bu$ for the hours at which power flow circulates through each line. Eq. (46) represents the *line - output bus factor*, calculated as the ratio between the sum of power flows which are leaving the bus $bu_o = bu$ through line l, and the sum of power flows from all lines which are leaving the common bus $bu_o = bu$.

$$\frac{\sum_{t\ /\ p\_l_{l,t,bu}\neq 0} p\_l_{l,t,bu}}{\sum_{t\ /\ p\_l_{l,t,bu}\neq 0} \bar{F}_l}\quad l = 1,\ \ldots, L;;\ \ bu = 1,\ \ldots, BU \qquad (44)$$

$$\frac{\sum_{t\ /\ p\_l_{l,t,bu}\neq 0} p\_l_{l,t,bu_i=bu}}{\sum_{t\ /\ p\_l_{l,t,bu}\neq 0} \sum_{l=1}^{l=L} p\_l_{l,t,bu_i=bu}},\quad l = 1,\ \ldots, L;\ \ bu_i = 1,\ \ldots, BU; \qquad (45)$$

$$\frac{\sum_{t\ /\ p\_l_{l,t,bu}\neq 0} p\_l_{l,t,bu_o=bu}}{\sum_{t\ /\ p\_l_{l,t,bu}\neq 0} \sum_{l=1}^{l=L} p\_l_{l,t,bu_o=bu}},\quad l = 1,\ \ldots, L;;\ \ bu_o = 1,\ \ldots, BU \qquad (46)$$

Each point in the ordinate axis of Fig. 9 matches to two points on the abscissa axis: the point corresponding to the bus where the power flow comes in and the point where the power flow comes out.

In this figure, two main zones where delimited by the value of 0.5 for the three factors. The zone in the upper right side is called *high performing zone*. In this zone the lines and buses are near full capacity; meaning a good utilization of the lines. High performing

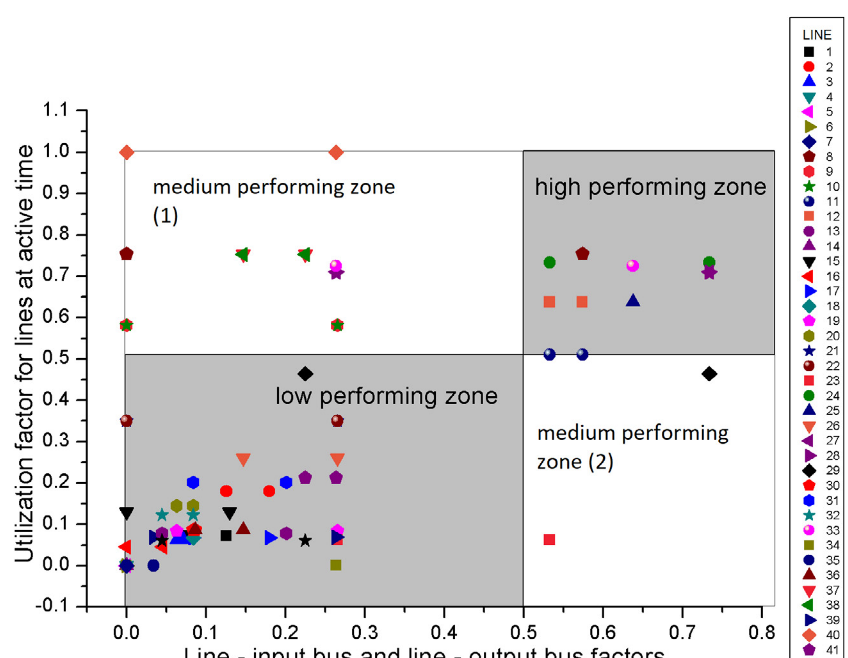

Fig. 9. 31- bus power system. Line performance per bus.

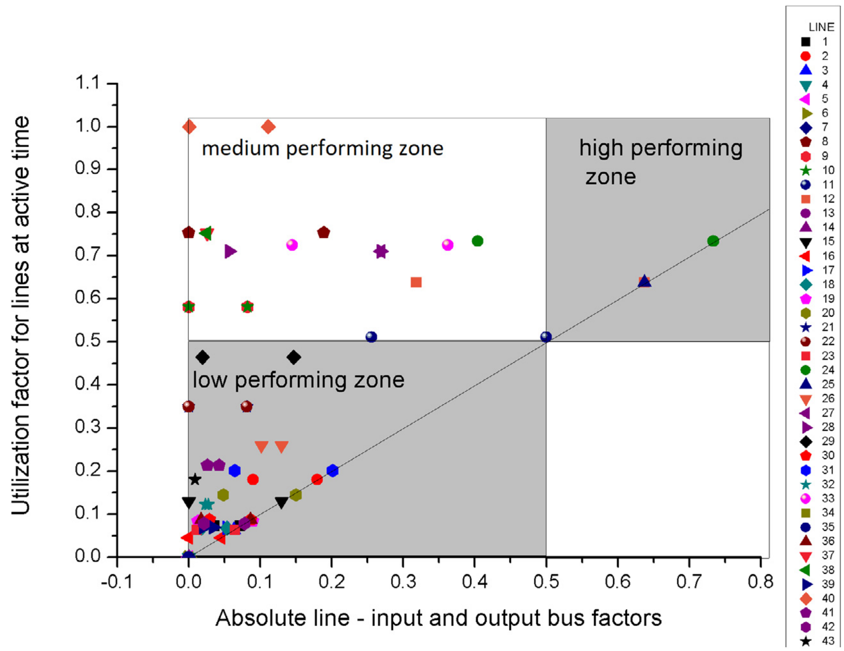

Fig. 10. 31-bus power system. Line performances according to their maximum capacities.

zone includes lines 8, 11, 12, 24, 25, 33, 38, and 39. Lines belonging to this zone are important for power system and the operator must pay particular attention to the maintenance of them. If one of these lines fails, some problems might arise as line overloads, increasing of total cost, and even the impossibility of transmitting power flows to loads.

The other area delimited is in the lower left side; this area indicates low use of lines compared to its maximum capacity and is called *low performing zone*. The vast majority of lines are located in this zone; that is lines 1–7, 9, 13–15, 17–22, 26–28, 30–32, 34, 36, and 41–43. Lines belonging to the low performing zone have power flow values that are very low, in comparison with the line limits. And the power flow values are also low, when the sum of power flow of all lines which are connected to the same bus is considered. The zone on the upper left-hand side of the figure (labeled as *medium performing zone(1)*) corresponds to lines 10, 16, 35, 37 and 40. These lines have power flows close to the maximum that they can support, but their participation in the total power flow entering or exiting the buses is low. Finally, in the zone on the bottom right of the figure (labeled as *medium performing zone(2)*) are lines 29 and 23. These lines have power flows with values lower than the 50% of the maximum they can support. However, while lines 29 and 33 have low values for the line utilization factor, they present elevated values of *line – output bus factor* (higher than 0.5). This means that the power flows of these two lines represent 54% and 75% of the total power flows leaving buses 18 and 31, respectively. Given the aforementioned facts, lines 23 and 29 represent a secondary importance due to low values for this factor. This means that if there is any damage in one of these two lines, the power flow which is transmitted by lines 23 and 29 can be transmitted by other lines. For example, if there is an outage in line 23, the power flow of this line can be transmitted by the lines numbered as: 9, 10, 19, 21, 22, or 26 because these 6 lines also connect the bus 18, besides line 29. In addition, if there is an outage in line 29, the power flow of this line can be transmitted by lines: 37, 38, 41 or 43 because these 4 lines also connect the bus 31. In view of that, a damage in lines belonging to the medium performance zones are not so critical as in the case of lines which belong to the high performing zone. Lines of the medium zones must be receive maintenance primarily, in comparison with lines of the low performing zone

Fig. 9 allows to identify lines at which the system operators should focus special attention. Certainly, lines in the high performing zone are supporting elevated power flows, are near their full capacities and are crucial for the interconnected buses. These lines are susceptible to present a technical problem as overloads or outages if power flows exceed their maximum capacities, affecting significantly the whole system.

In Fig. 10, the participation of line l is compared to the sum of all maximum power flows of lines connected to the same bus. Similar to Fig. 9, *utilization factor for lines at hours with power flows* (Eq. (44)) is in the ordinate axis and each point in this axis is matched to two points on the axis of abscissas.

In abscissa axis, *absolute line - input/output bus factors* are depicted Eqs. (47) and ((48)). The factor computed in Eq. (47) represents the sum of power flows of line l entering the bus bu_i for the hours at which power flow circulates through each line, divided by the sum of maximum power flows of all lines which are entering the common bus bu_i during 24 h. Abscissa axis also presents the factor computed in Eq. (48); it represents the sum of power flows of line l leaving the bus bu_o at the hours at which power flow circulates through each line, divided by the sum of maximum power flows of all lines which are leaving the common bus bu_o during 24 h.

$$\frac{\sum_{t\ /\ p\_l_{l,t,bu}\neq 0} p\_l_{l,t,bu_i=bu}}{\sum_{l=1}^{l=L} \bar{F}_{l,bu_i=bu} * 24}, \quad l=1,\ \ldots,L;\ bu_i=1,\ \ldots,BU; \tag{47}$$

$$\frac{\sum_{t\ /\ p\_l_{l,t,bu}\neq 0} p\_l_{l,t,bu_o=bu}}{\sum_{l=1}^{l=L} \bar{F}_{l,bu_o=bu} * 24}, \quad l=1,\ \ldots,L;\ bu_o=1,\ \ldots,BU; \tag{48}$$

Three zones are delimited in Fig. 10: *high, medium* and *low performance zones.*

In the low performance zone are located those points having values for *utilization factor for lines at hours with power flows and absolute line- input/output bus factors,* (Eqs. (44), (47), and (48)) lower than 0.5. For the system analyzed, lines 1–7, 13–23, 26, 29–32, 34–36, 39, and 41–43 belong to this zone. A few lines have values of the aforementioned factors over 0.5, indicating a high participation in the programming of the system: lines 12, 24, and 25. These points are located in the high performance zone. These three lines are used most of the time periods and their power flows are close to the sum of maximum power flow capacities of all lines connected to the common bus *bu*. Therefore, an outage on one of these lines would lead to resort to other units, increasing the production costs or even that the system cannot fulfill the forecast demand.

Finally, there are 11 lines with values over 0.5 for *utilization factor for lines at hours with power flows* Eq. (44)) and lower 0.5 for *absolute line- input/output bus factors* (Eqs. (47) and ((48)): lines 8–11, 24, 27, 28, 33, 37, 38 and 40. The points belonging to these 11 lines are located in the medium performance zone. Power flows of these lines are close to their maximum capacities, but they are low compared to the sum of maximum power flow capacities of all lines connected to the common bus *bu*. These lines are secondary in relation to the power flows that connected buses can support. Hence, these lines are crucial for power system only if buses are not connected by any other line.

Therefore, lines of the high performance zone are crucial. These lines are operating near their full capacities and an outage on any of them will cause serious consequences for the whole system, since through these lines flow most of the power that the connected bus transmit, produce, or consume. Consequently, lines in the high performance zone must be correctly and constantly maintained.

5.3. IEEE 118-bus system

Comparing results of UC and SCUC (DC model) problems, it can be appreciated that the increase of 6.3% due to the inclussion of transmission constraints.

Regarding the advantages of including variables $y_{l,t}$ in transmission constraints, the comparison between the classical DC model and the model proposed here indicate that the reductions of up to 4.2% in the total cost is due to the fact that the proposed model can reach solutions that are unavailable for the classic DC model. The fact that there are 930 more time periods with inactive lines than case 4.3.2 constitutes other advantage. When the scheduling of an electric system belonging to a big city or a country is considered, the technical benefits could be important and the economic benefits could represent the savings of millons of dollars.

6. Conclusions

In this paper, a new approach for modeling transmission constraints in Security Constrained Unit Commitment Problems based on DC power flow model is presented. This approach solves the scheduling of generators in power systems taking into account transmission constraints. In fact, transmission constraints are modeled incorporating binary variables. Novel model includes four equations for each line. But by implementing of binary variables, these equations can be activated or deactivated in order to achieve better solutions.

Three systems are solved by applying the proposed approach. Comparisons with the classical DC power flow are also presented. The numerical tests demonstrate the effectiveness of the proposed approach. For the three systems tested, the optimal solutions obtained with the proposed model present costs considerably lower than the ones obtained with the classic DC power flow model. This also illustrates that the presented model is capable of representing more solutions than the classical model; then by applying the proposed approach it is possible to find solutions more economic for satisfying the required demand.

Finally, additional information obtained from the solutions of SCUC problems is presented trough graphics. This information is very helpful to improve the system operation through the use of new indexes as the utilization and commitment factors for generating units, utilization factor for transmission lines, utilization factor for lines at active times and relative and absolute line-bus factors. Thus, lines and generating units critical for the system can be identified, assisting the operator in deciding maintenance of the system, productivity, and investments in technical facilities.

Acknowledgments

This work was supported by Consejo Nacional de Investigaciones Científicas y Técnicas CONICET (PIP no. 11220130100606), Ministerio de Ciencia, Tecnología e Innovación Productiva MINCYT (PICT no. 3458).

Appendix A. 6-bus power system.

Table A1

Table A1
Case 4.1.2. and 4.1.3. Transmission limits per line.

Line number	Power limit [MW]
1	80
2	100
3	60
4	15
5	60
6	10
7	30
8	20
9	50
10	15
11	10

Appendix B. 118-bus power system

Tables B1–B4

Table B1
IEEE 118 bus system. Data for 54 thermal units.

Unit	Bus no	Unit cost coefficients			Pmax	Pmin	I.stat	Min Dn	Min Up	Ramp up	Ramp down	Start up
		a [$/MWh^2]	b [$/MWh]	c [$]	[MW]	[MW]	[h]	[h]	[h]	[MW/h]	[MW/h]	[$]
1	4	0.06966	26.24382	31.67	30	5	−1	1	1	15	15	40
2	6	0.06966	26.24382	31.67	30	5	−1	1	1	15	15	40
3	8	0.06966	26.24382	31.67	30	5	−1	1	1	15	15	40
4	10	0.01088	12.8875	6.78	300	150	−8	8	8	50	50	440
5	12	0.01088	12.8875	6.78	300	100	−8	8	8	150	150	110
6	15	0.06966	26.24382	31.67	30	10	−1	1	1	150	150	40
7	18	0.01280	17.82	10.15	100	25	−5	5	5	50	50	50
8	19	0.06966	26.24382	31.67	30	5	−1	1	1	15	15	40
9	24	0.06966	26.24382	31.67	30	5	−1	1	1	15	15	40
10	25	0.01088	12.8875	6.78	300	100	−8	8	8	150	150	100
11	26	0.00300	10.76	32.96	350	100	−8	8	8	175	175	100
12	27	0.06966	26.24382	31.67	30	8	−1	1	1	15	15	40
13	31	0.06966	26.24382	31.67	30	8	−1	1	1	15	15	40
14	32	0.01280	17.82	10.15	100	25	−5	5	5	50	50	50
15	34	0.06966	26.24382	31.67	30	8	−5	5	5	15	15	40
16	36	0.01280	17.82	10.15	100	25	−1	1	1	50	50	50
17	40	0.06966	26.24382	31.67	30	8	−5	5	5	15	15	40
18	42	0.06966	26.24382	31.67	30	8	−1	1	1	15	15	40
19	46	0.01280	17.82	10.15	100	25	−1	1	1	50	50	59
20	49	0.00240	12.3299	99 28	250	50	−5	5	5	125	125	100
21	54	0.00240	12.3299	99 28	250	50	−8	8	8	125	125	100
22	55	0.01280	17.82	10.15	100	25	−8	8	8	50	50	50
23	56	0.01280	17.82	10.15	100	25	−5	5	5	50	50	50
24	59	0.00440	13.29	39	200	50	−5	5	5	100	100	100
25	61	0.00440	13.29	39	200	50	−10	10	10	100	100	100
26	62	0.01280	17.82	10.15	100	25	−10	10	10	50	50	50
27	65	0.01059	8.339148	64.16	420	100	−5	5	5	210	210	250
28	66	0.01059	8.339148	64.16	420	100	−10	10	10	210	210	250
29	69	0.01088	12.8875	6.78	300	80	−10	10	10	150	150	100
30	70	0.04592	15.47077	74.33	80	30	−10	10	10	40	40	45
31	72	0.06966	26.24382	31.67	30	10	−4	4	4	15	15	40
32	73	0.06966	26.24382	31.67	30	5	−1	1	1	15	15	40
33	74	0.02830	37.69679	17.95	20	5	−1	1	1	10	10	30
34	76	0.01280	17.82	10.15	100	25	−1	1	1	50	50	50
35	77	0.01280	17.82	10.15	100	25	−5	5	5	50	50	50
36	80	0.01088	12.8875	6.78	300	150	−5	5	5	150	150	440
37	82	0.01280	17.82	10.15	100	25	−10	10	10	50	50	50
38	85	0.06966	26.24382	31.67	30	10	−5	5	5	15	15	40
39	87	0.00300	10.76	32.96	300	100	−1	1	1	150	150	440
40	89	0.01088	12.8875	6.78	200	50	−10	10	10	100	100	400
41	90	0.02830	37.69679	17.95	20	8	−10	10	10	10	10	30
42	91	0.00977	22.94226	58.81	50	20	−1	1	1	25	25	45
43	92	0.01088	12.8875	6.78	300	100	−1	1	1	150	150	100
44	99	0.01088	12.8875	6.78	300	100	−8	8	8	150	150	100
45	100	0.01088	12.8875	6.78	300	100	−8	8	8	150	150	110
46	103	0.02830	37.69679	17.95	20	8	−8	8	8	10	10	30
47	104	0.01280	17.82	10.15	100	25	−1	1	1	50	50	50
48	105	0.01280	17.82	10.15	100	25	−5	5	5	50	50	50
49	107	0.02830	37.69679	17.95	20	8	−5	5	5	10	10	30
50	110	0.00977	22.94226	58.81	50	25	−1	1	1	25	25	45
51	111	0.01280	17.82	10.15	100	25	−2	2	2	50	50	50
52	112	0.01280	17.82	10.15	100	25	−5	5	5	50	50	50
53	113	0.01280	17.82	10.15	100	25	−5	5	5	50	50	50
54	116	0.00977	22.94226	58.81	50	25	−2	2	2	25	25	45

Table B2
IEEE 118 bus system. Data for 186 lines.

Line	From bus	To bus	x [p.u.]	Limit [MW]	Line	From bus	To bus	x [p.u.]	Limit [MW]	Line	From bus	To bus	x [p.u.]	Limit [MW]
1	1	2	0.0999	175	63	46	47	0.127	175	125	79	80	0.0704	175
2	1	3	0.0424	175	64	46	48	0.189	175	126	68	81	0.0202	500
3	4	5	0.00798	500	65	47	49	0.0625	175	127	81	80	0.037	500
4	3	5	0.108	175	66	42	49	0.323	175	128	77	82	0.0853	200
5	5	6	0.054	175	67	42	49	0.323	175	129	82	83	0.03665	200
6	6	7	0.0208	175	68	45	49	0.186	175	130	83	84	0.132	175
7	8	9	0.0305	500	69	48	49	0.0505	175	131	83	85	0.148	175
8	8	5	0.0267	500	70	49	50	0.0752	175	132	84	85	0.0641	175
9	9	10	0.0322	500	71	49	51	0.137	175	133	85	86	0.123	500
10	4	11	0.0688	175	72	51	52	0.0588	175	134	86	87	0.2074	500
11	5	11	0.0682	175	73	52	53	0.1635	175	135	85	88	0.102	175
12	11	12	0.0196	175	74	53	54	0.122	175	136	85	89	0.173	175
13	2	12	0.0616	175	75	49	54	0.289	175	137	88	89	0.0712	500
14	3	12	0.16	175	76	49	54	0.291	175	138	89	90	0.188	500
15	7	12	0.034	175	77	54	55	0.0707	175	139	89	90	0.0997	500
16	11	13	0.0731	175	78	54	56	0.00955	175	140	90	91	0.0836	175
17	12	14	0.0707	175	79	55	56	0.0151	175	141	89	92	0.0505	500
18	13	15	0.2444	175	80	56	57	0.0966	175	142	89	92	0.1581	500
19	14	15	0.195	175	81	50	57	0.134	175	143	91	92	0.1272	175
20	12	16	0.0834	175	82	56	58	0.0966	175	144	92	93	0.0848	175
21	15	17	0.0437	500	83	51	58	0.0719	175	145	92	94	0.158	175
22	16	17	0.1801	175	84	54	59	0.2293	175	146	93	94	0.0732	175
23	17	18	0.0505	175	85	56	59	0.251	175	147	94	95	0.0434	175
24	18	19	0.0493	175	86	56	59	0.239	175	148	80	96	0.182	175
25	19	20	0.117	175	87	55	59	0.2158	175	149	82	96	0.053	175
26	15	19	0.0394	175	88	59	60	0.145	175	150	94	96	0.0869	175
27	20	21	0.0849	175	89	59	61	0.15	175	151	80	97	0.0934	175
28	21	22	0.097	175	90	60	61	0.0135	500	152	80	98	0.108	175
29	22	23	0.159	175	91	60	62	0.0561	175	153	80	99	0.206	200
30	23	24	0.0492	175	92	61	62	0.0376	175	154	92	100	0.295	175
31	23	25	0.08	500	93	63	59	0.0386	500	155	94	100	0.058	175
32	26	25	0.0382	500	94	63	64	0.02	500	156	95	96	0.0547	175
33	25	27	0.163	500	95	64	61	0.0268	500	157	96	97	0.0885	175
34	27	28	0.0855	175	96	38	65	0.0986	500	158	98	100	0.179	175
35	28	29	0.0943	175	97	64	65	0.0302	500	159	99	100	0.0813	175
36	30	17	0.0388	500	98	49	66	0.0919	500	160	100	101	0.1262	175
37	8	30	0.0504	175	99	49	66	0.0919	500	161	92	102	0.0559	175
38	26	30	0.086	500	100	62	66	0.218	175	162	101	102	0.112	175
39	17	31	0.1563	175	101	62	67	0.117	175	163	100	103	0.0525	500
40	29	31	0.0331	175	102	65	66	0.037	500	164	100	104	0.204	175
41	23	32	0.1153	140	103	66	67	0.1015	175	165	103	104	0.1584	175
42	31	32	0.0985	175	104	65	68	0.016	500	166	103	105	0.1625	175
43	27	32	0.0755	175	105	47	69	0.2778	175	167	100	106	0.229	175
44	15	33	0.1244	175	106	49	69	0.324	175	168	104	105	0.0378	175
45	19	34	0.247	175	107	68	69	0.037	500	169	105	106	0.0547	175
46	35	36	0.0102	175	108	69	70	0.127	500	170	105	107	0.183	175
47	35	37	0.0497	175	109	24	70	0.4115	175	171	105	108	0.0703	175
48	33	37	0.142	175	110	70	71	0.0355	175	172	106	107	0.183	175
49	34	36	0.0268	175	111	24	72	0.196	175	173	108	109	0.0288	175
50	34	37	0.0094	500	112	71	72	0.18	175	174	103	110	0.1813	175
51	38	37	0.0375	500	113	71	73	0.0454	175	175	109	110	0.0762	175
52	37	39	0.106	175	114	70	74	0.1323	175	176	110	111	0.0755	175
53	37	40	0.168	175	115	70	75	0.141	175	177	110	112	0.064	175
54	30	38	0.054	175	116	69	75	0.122	500	178	17	113	0.0301	175
55	39	40	0.0605	175	117	74	75	0.0406	175	179	32	113	0.203	500
56	40	41	0.0487	175	118	76	77	0.148	175	180	32	114	0.0612	175
57	40	42	0.183	175	119	69	77	0.101	175	181	27	115	0.0741	175
58	41	42	0.135	175	120	75	77	0.1999	175	182	114	115	0.0104	175
59	43	44	0.2454	175	121	77	78	0.0124	175	183	68	116	0.00405	500
60	34	43	0.1681	175	122	78	79	0.0244	175	184	12	117	0.14	175
61	44	45	0.0901	175	123	77	80	0.0485	500	185	75	118	0.0481	175
62	45	46	0.1356	175	124	77	80	0.105	500	186	76	118	0.0544	175

Table B3
IEEE 118 bus system. Data for total hourly loads.

Hour	Load [MW]	Hour	Load [MW]	Hour	Load [MW]	Hour	Load [MW]
1	3314.4	7	3314.4	13	4073.6	19	5136.4
2	3010.72	8	3921.76	14	3769.9	20	5440.1
3	2403.36	9	4225.44	15	4680.9	21	5592
4	1036.8	10	4680.9	16	4832.8	22	4832.8
5	1796	11	4756.8	17	4453.2	23	4605
6	2555.2	12	4377.2	18	4756.8	24	4225.4

Table B4
IEEE 118 bus system. Participation per bus in the total load [in percent].

Bus no	Load [%]	Bus no	Load [%]	Bus no	Load [%]	Bus no	Load [%]	Bus no	Load [%]
1	1.45	25	0.00	49	2.33	73	0.00	97	0.40
2	0.57	26	0.00	50	0.46	74	1.82	98	0.91
3	1.11	27	1.76	51	0.46	75	1.26	99	0.00
4	0.85	28	0.48	52	0.48	76	1.82	100	0.99
5	0.00	29	0.68	53	0.62	77	1.63	101	0.59
6	1.48	30	0.00	54	3.03	78	1.90	102	0.13
7	0.54	31	1.22	55	1.69	79	1.04	103	0.62
8	0.00	32	1.68	56	2.25	80	3.48	104	1.02
9	0.00	33	0.65	57	0.32	81	0.00	105	0.83
10	0.00	34	1.68	58	0.32	82	1.45	106	1.15
11	1.99	35	0.94	59	7.42	83	0.54	107	0.75
12	1.34	36	0.88	60	2.09	84	0.29	108	0.05
13	0.97	37	0.00	61	0.00	85	0.64	109	0.21
14	0.40	38	0.00	62	2.06	86	0.56	110	1.04
15	2.56	39	0.72	63	0.00	87	0.00	111	0.00
16	0.71	40	0.54	64	0.00	88	1.29	112	0.67
17	0.31	41	0.99	65	0.00	89	0.00	113	0.00
18	1.71	42	0.99	66	1.04	90	2.09	114	0.23
19	1.28	43	0.48	67	0.75	91	0.00	115	0.63
20	0.51	44	0.43	68	0.00	92	1.74	116	0.00
21	0.40	45	1.42	69	0.00	93	0.32	117	0.57
22	0.28	46	0.75	70	1.77	94	0.80	118	0.88
23	0.20	47	0.91	71	0.00	95	1.13		
24	0.00	48	0.54	72	0.00	96	1.02		

References

Abdul-Rahman, K.H., Shahidehpour, S.M., Aganacic, M., Mokhtari, S., 1996. A practical resource scheduling with OPF constraints. IEEE Trans. Power Syst. 11, 254–259. doi:10.1109/59.486103.

Alvarez, G., Marcovecchio, M., Aguirre, P., 2016. Unit commitment scheduling including transmission constraints: a MILP formulation. In: Computer Aided Chemical Engineering. Elsevier Masson SAS, pp. 2157–2162. doi:10.1016/B978-0-444-63428-3.50364-7.

Badakhshan, S., Kazemi, M., Ehsan, M., 2015. Security constrained unit commitment with flexibility in natural gas transmission delivery. J. Nat. Gas Sci. Eng. 27, 632–640. doi:10.1016/j.jngse.2015.09.011.

Bai, Y., Zhong, H., Xia, Q., Kang, C., Xie, L., 2015. A decomposition method for network-constrained unit commitment with AC power flow constraints. Energy 88, 595–603. doi:10.1016/j.energy.2015.05.082.

Carrión, M., Arroyo, J.M., 2006. A computationally efficient mixed-integer linear formulation for the thermal unit commitment problem. IEEE Trans. Power Syst. 21, 1371–1378. doi:10.1109/TPWRS.2006.876672.

Castillo, E., Conejo, A.J., Pedregal, P., Garcia, R., Alguacil, N., 2002. Building and Solving Mathematical Programming Models in Engineering and Science. John Wiley & Sons.

Fu, Y., Shahidehpour, M., Li, Z., 2005. Security-constrained unit commitment with AC constraints *. IEEE Trans. Power Syst. 20, 1538–1550. doi:10.1109/TPWRS.2005.854375.

Grey, A., Sekar, A., 2008. Unified solution of security-constrained unit commitment problem using a linear programming methodology. IET Gener. Transm. Distrib. 2, 856–867. doi:10.1049/iet-gtd.

Guan, X., Guo, S., Zhai, Q., 2005. The conditions for obtaining feasible solutions to security-constrained unit commitment problems. IEEE Trans. Power Syst. 20, 1746–1756. doi:10.1109/TPWRS.2005.857399.

Guan, X., Zhai, Q., Papalexopoulos, A., 2003. Optimization based methods for unit commitment: Lagrangian relaxation versus general mixed integer programming. In: Power Engineering Society General Meeting, 2. IEEE, pp. 1095–1100. doi:10.1109/PES.2003.1270468.

Guo, S., 2012. A quick method for judging the feasibility of security-constrained unit commitment problems within lagrangian relaxation framework *. Energy Power Eng. 4, 432–438. doi:10.4236/epe.2012.46057.

Guy, J.D., 1971. Security constrained unit commitment. IEEE Trans. Power Appar. Syst. PAS-90 1385–1390. doi:10.1109/TPAS.1971.292942.

Illinois Center for a Smarter Electric Grid. IEEE 118-Bus System accessed 3.17.16.

International Energy Agency, (2014). 2014 Key World Energy Statistics. Paris.

Kazarlis, S.A., Bakirtzis, A.G., Petridis, V., 1996. A genetic algorithm solution to the unit commitment problem. IEEE Trans. Power Syst. 11, 83–92. doi:10.1109/59.485989.

Lotfjou, A., Shahidehpour, M., Fu, Y., 2010. Security-constrained unit commitment with AC / DC transmission systems. IEEE Trans. Power Syst. 25, 531–542. doi:10.1109/TPWRS.2009.2036486.

Lowery, P.G., 1966. Generating unit commitment by dynamic programming. IEEE Trans. Power Appar. Syst. PAS-85 422–426. doi:10.1109/TPAS.1966.291679.

Marcovecchio, M.G., Novais, A.Q., Grossmann, I.E., 2014. Deterministic optimization of the thermal unit commitment problem: a branch and cut search. Comput. Chem. Eng. 67, 53–68. doi:10.1016/j.compchemeng.2014.03.009.

Naidoo, R.D., 2007. A mixed integer programming formulation of generator startup costs. In: Proceedings of the International Power Engineering Conference, pp. 173–176.

Oonsivilai, A., Marungsri, B., Barsoum, N., Uatrongjit, S., Vasant, P., 2008. Solving the unit commitment problem using an adaptive immune genetic algorithm. AIP Conf. Proc. 1052, 256–262. doi:10.1063/1.3008677.

Ostrowski, J., Anjos, M.F., Vannelli, A., 2012. Tight mixed integer linear programming formulations for the unit commitment problem. IEEE Trans. Power Syst. 27, 39–46. doi:10.1109/TPWRS.2011.2162008.

Overbye, T.J., Cheng, X., Sun, Y., 2004. A comparison of the AC and DC power flow models for LMP calculations. In: Proceedings of the 37th Annual Hawaii International Conference on System Sciences. IEEE, p. 9. doi:10.1109/HICSS.2004.1265164.

Padhy, N.P., 2004. Unit commitment — a bibliographical survey. IEEE Trans. Power Syst. 19, 1196–1205. doi:10.1109/TPWRS.2003.821611.

Quan, H., Srinivasan, D., Khambadkone, A.M., Khosravi, A., 2015. A computational framework for uncertainty integration in stochastic unit commitment with intermittent renewable energy sources. Appl. Energy 152, 71–82. doi:10.1016/j.apenergy.2015.04.103.

Reza Norouzi, M., Ahmadi, A., Esmaeel Nezhad, A., Ghaedi, A., 2014. Mixed integer programming of multi-objective security-constrained hydro/thermal unit commitment. Renew. Sustain. Energy Rev. 29, 911–923. doi:10.1016/j.rser.2013.09.020.

Ruzic, S., Rajakovic, N., 1991. A new approach for solving extended unit commitment problem. IEEE Trans. Power Syst. doi:10.1109/59.131072.

Saidi, K., Hammami, S., 2015. The impact of CO2 emissions and economic growth on energy consumption in 58 countries. Energy Rep. 1, 62–70. doi:10.1016/j.egyr.2015.01.003.

Senthil Kumar, V., Mohan, M.R., 2010. Solution to security constrained unit commitment problem using genetic algorithm. Int. J. Electr. Power Energy Syst. 32, 117–125. doi:10.1016/j.ijepes.2009.06.019.

Shafiee, S., Topal, E., 2009. When will fossil fuel reserves be diminished? Energy Policy 37, 181–189. doi:10.1016/j.enpol.2008.08.016.

Shaw, J.J., 1995. Direct method for security-constrained unit commitment. IEEE Trans. Power Syst. 10, 1329–1342. doi:10.1109/59.466520.

Stagg, W., El-Abiad, A.H., 1968. Computer Methods in Power System Analysis. McGraw-Hill.

Stott, B., Jardim, J., Alsac, O., 2009. DC Power Flow Revisited. IEEE Trans. Power Syst. 24, 1290–1300. doi:10.1109/TPWRS.2009.2021235.

Tseng, C., Guan, X., Svoboda, A.J., 1998. Multi-area unit commitment for large-scale power systems. IEE Proc. Gener. Transm. Distrib. 145, 415–421. doi:10.1049/ip-gtd:19981987.

Tseng, C., Oren, S.S., Cheng, C.S., Li, C., Svoboda, A.J., Johnson, R.B., 1999. A transmission-constrained unit commitment method in power system scheduling. Decis. Support Syst. 24, 297–310. doi:10.1016/S0167-9236(98)00072-4.

Van Den Bergh, K., Delarue, E., & D'haeseleer, W. (2014). DC power flow in unit commitment models. *TME Work. Pap. Environ. Tech. Rep.*

Vielma, J.P., 2015. Mixed integer linear programming formulation techniques. SIAM Rev. 57, 3–57. doi:10.1137/130915303.

Wang, J., Shahidehpour, M., Li, Z., Member, S., 2009. Contingency-constrained reserve requirements in joint energy and ancillary services auction. IEEE Trans. POWER Syst. 24, 1457–1468. doi:10.1109/TPWRS.2009.2022983.

Wright, B., 2013. A review of unit commitment. Columbia Eng. 1–14.

Yamin, H.Y., 2004. Review on methods of generation scheduling in electric power systems. Electr. Power Syst. Res. 69, 227–248. doi:10.1016/j.epsr.2003.10.002.

Yan, P., Sekar, A., 2005. Steady-state analysis of power system having multiple FACTS devices using line-flow-based equations. IEE Proc. Gener. Transm. Distrib 151, 31–39. doi:10.1049/ip-gtd:20041133.

Zhai, Q., Guan, X., Yang, J., 2009. Fast unit commitment based on optimal linear approximation to nonlinear fuel cost: error analysis and applications. Electr. Power Syst. Res. 79, 1604–1613. doi:10.1016/j.epsr.2009.06.005.

Zhao, F., Luh, P.B., Yan, J.H., Stern, G.A., Chang, S.C., 2008. Payment cost minimization auction for deregulated electricity markets with transmission capacity constraints. IEEE Trans. Power Syst. 23, 532–544. doi:10.1109/TPWRS.2008.919404.

Zhu, J., 2009. Optimization of Power System Operation. John Wiley & Sons, Hoboken, NJ doi:10.1002/9780470466971.